Available online at www.sciencedirect.com

ScienceDirect

journal homepage: www.elsevier.com/locate/he

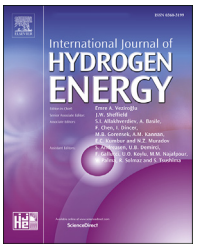

Direct numerical simulations of auto-igniting mixing layers in ammonia and ammonia-hydrogen combustion under engine-relevant conditions

W. Yang [a], K.K.J. Ranga Dinesh [b,*], K.H. Luo [c,**], D. Thévenin [d]

[a] Center for Combustion Energy, Department of Energy and Power Engineering, Tsinghua University, 10084, Beijing, China

[b] Energy Technology Research Group, School of Engineering, Faculty of Engineering and Physical Sciences, University of Southampton, Southampton, SO17 1BJ, UK

[c] Department of Mechanical Engineering, University College London, Torrington Place, London WC1E 7JE, UK

[d] Laboratory of Fluid Dynamics and Technical Flows, University of Magdeburg "Otto von Guericke", Universitatsplatz 2, D-39106 Magdeburg, Germany

HIGHLIGHTS

- DNS study of auto-ignition in ammonia and ammonia-hydrogen combustion.
- Elevated pressure and hydrogen addition accelerate the auto-ignition process.
- Induction and thermal runaway stages are identified.
- The radicals NH_2, OH, HNO distinguish the entire auto-ignition process.

ARTICLE INFO

Article history:
Received 15 July 2022
Received in revised form
28 August 2022
Accepted 30 August 2022
Available online xxx

Keywords:
Direct numerical simulation
Ammon-hydrogen-air mixing layers
Auto-ignition
High turbulence
Elevated pressure

ABSTRACT

This study investigated auto-ignition characteristics of ammonia-air and ammonia-hydrogen-air laminar and turbulent mixing layers by means of direct numerical simulations (DNS) under elevated pressure conditions. The results show that elevated pressure and hydrogen addition accelerate the auto-ignition process, reducing the auto-ignition delay time. Analysis of the heat release rate revealed that the first peak of the heat release rate corresponds to the increment of appearance in temperature (induction stage) and the second peak of the heat release rate corresponds to the steady maximum temperature regime (thermal runaway stage). The results found that both induction and thermal runaway stages are affected by turbulence for pure ammonia-air mixing layers, while only the thermal runaway stage is affected by turbulence for ammonia-hydrogen-air mixing layers. The auto-ignition occurs along the most reactive mixture fraction with lower scalar dissipation rate, being further reduced by elevated pressure and hydrogen addition. Three radicals (NH_2, OH, HNO) distinguish the entire auto-ignition process very well for all cases.

* Corresponding author.
** Corresponding author.
E-mail addresses: dinesh.kahanda-koralage@soton.ac.uk (K.K.J. Ranga Dinesh), k.luo@ucl.ac.uk (K.H. Luo).

https://doi.org/10.1016/j.ijhydene.2022.08.290

Introduction

The combustion of ammonia (NH_3) as an alternative and zero-carbon fuel has received much attention in recent years. For example, Kobayashi et al. [1] and Valera-Medina et al. [2] published detailed literature addressing fundamental and applied research on ammonia combustion. Ammonia can be considered as an efficient hydrogen-energy-carrier because of the 17.6% (by mass) gravimetric hydrogen (H_2) density. Ammonia is much more easily liquefied and stored in ambient temperature (25 °C) under only 9.9 atm or −33.4 °C at atmospheric condition, resulting in economic and secure transport compared to hydrogen. However, the combustion of ammonia presents some technical challenges when it burns in combustion applications such as internal combustion engine and gas turbine engine either in premixed combustion mode or non-premixed (diffusion) combustion mode. It has a weak burning intensity (only 0.07 m/s of maximum laminar flame speed), a low heating value (18.6 MJ/kg) and a high auto-ignition temperature (650 °C), all of them make it harder to combust pure ammonia in compression ignition, spark ignition and gas turbine engines under conventional operating conditions. To tackle this issue, blending ammonia with combustion promoters such as hydrogen which is well known for its high reactivity, was investigated in the literature.

Since ammonia is becoming a potentially important fuel for internal combustion engines and gas turbine engines for transportation and power generation applications, fundamental study of auto-ignition (or spontaneous ignition or self-ignition) characteristics of ammonia and ammonia fuel blends under engine relevant conditions is critically important for its utilisation in combustion engines operate with turbulent non-premixed and partially premixed combustion modes. The auto-ignition is characterised by the transition from slowly reacting state to a fully burning state with gradual temperature increase and occurs away from stoichiometry at a most reactive mixture fraction, which can be evaluated from homogenous or laminar flow auto-ignition calculations, and at locations in the turbulent flow with low scalar dissipation such as the cores of vortices. For example, Mastorakos [3] carried out a thorough review on the auto-ignition of non-premixed turbulent combustion with respect to four different canonical ignition configurations: turbulent fuel jet into oxidizer, mixing layer, counter-flow and the partially mixing state of compression ignition in a conventional diesel engine.

In auto-ignition investigations of laminar flames, the counter-flow is the most widely used by combining the fuel at standard temperature and the hot oxidizer. The work carried out by Liñán [4] illustrated the relationship between the flame temperature and the Damköhler number corresponds to auto-ignition by the S-shaped plot, showing a shift from frozen to a burning state. Hydrogen [5], methane (CH_4) [6], syngas (H_2/CO) [7], and other hydrocarbon fuels, such as dimethyl ether (DME) [8] were studied to derive the critical temperature as a function of the strain rate by following the strategy of Liñán [4]. In auto-ignition studies of turbulent flames, the fuel jet into oxidizer is commonly used to study auto-ignition features for different fuels. For example, Yu [9] has carried out the asymptotic and numerical analyses of hydrogen ignition of a fuel jet in a supersonic airstream in which he extended the theory derived by Liñán and Crespo [10]. Arndt et al. [11] experimentally studied the role of temperature, mixture fraction and scalar dissipation rate on transient methane fuel injection by using the auto-ignition in a jet into hot co-flow burner and concluded that it was not necessary to evaluate the complete transient fuel injection to study the onset of auto-ignition. Markides et al. [12] captured the hydrogen, acetylene and n-heptane auto-ignition and subsequent flame propagation by an intensified high-speed camera, which revealed the statistically steady random spots regime and the flashback regime.

The turbulent auto-ignition characteristics of hydrogen jet with heated co-flow were analysed experimentally by Markides et al. [13] and Echekki et al. [14], showing the delaying effects of turbulence on auto-ignition due to the scalar dissipation rate and turbulent stirring. Recently, DME has become another targeted fuel to investigate for two-stage auto-ignition owing to the negative temperature coefficient (NTC) auto-ignition regime. The turbulent jet of DME were examined experimentally and numerically. Bhagatwala et al. [15] exhibited the OH/CH_2O (formaldehyde) product imaging as the peak heat release rate marker compared with DNS results. Echekki et al. [16] also investigated the turbulence effects on auto-ignition of DME in turbulent co-flow jet. They observed that the auto-ignition would be delayed under higher temperature preheat air while the first-stage would be accelerated under lower temperature preheat air conditions. Macfarlane et al. [17] showed the evolution of auto-ignition kernels for experimental DME turbulent flames. Formation, growth, and final merging of DME kernels were performed by CH_2O and OH of PLIF method. Non-premixed ammonia-substituted hydrogen-air was studied by Um et al. [18], showing the combustion stability limits and NOx emissions under normal temperature and pressure conditions. Woo et al. [19] also investigated the NOx formation in laminar jet flames for ammonia and methane with oxidizer. They observed that the NOx formation appeared in the two ranges of either relatively low or high ratio of oxygen with the addition of ammonia.

Another fundamental non-premixed set up is the mixing layer configuration, which has been widely applied in numerical investigation of auto-ignition, even though the mixing layer is hardly possible to achieve in terms of experiments [3]. By using DNS, Mastorakos et al. [20] revealed that the first auto-ignition location would be almost independent of the turbulence time scale and the ignition delay time was longer than that in turbulent case. Also, the most reactive mixture fraction was defined where the auto-ignition occurred, which could be evaluated by the laminar simulation and only depended on the fuel and oxidizer temperatures and the activation energy. Hydrogen has been used to investigate the auto-ignition phenomenon in the mixing layer configuration. Different investigations were carried out to study the auto-ignition process of hydrogen due to its high reactivity, diffusivity and three different explosive limits at elevated pressures. Im et al. [21] studied the auto-ignition of hydrogen-air mixing layer with two-dimensional homogeneous turbulence. They found that the ignition delay time was not monotonic with an increasing turbulence intensity. Echekki et al. [22,23] have studied the role of elementary reactions and diffusion in auto-ignition of turbulent non-homogeneous hydrogen-air mixtures. Hilbert et al. [24] employed a more realistic chemistry and transport models

Please cite this article as: Yang W et al., Direct numerical simulations of auto-igniting mixing layers in ammonia and ammonia-hydrogen combustion under engine-relevant conditions, International Journal of Hydrogen Energy, https://doi.org/10.1016/j.ijhydene.2022.08.290

to study laminar and turbulent hydrogen-air mixing layers by means of DNS. Homogeneous mixing ignition (HMI) and laminar mixing ignition (LMI) were calculated to derive the most reactive mixture fraction. They observed that the hydrogen-air mixing layer always ignited faster under turbulence flow condition than laminar flow condition and the first ignition spot under turbulence condition would appear in the lowest scalar dissipation rate site along the most reactive mixture fraction iso-line. Chen et al. [25,26] also carried DNS of hydrogen-air mixture ignition problem. The thermal stratification and high-pressure conditions were set with detailed chemistry and transport models. Yao et al. [27,28] illustrated characteristics of the two-stage auto-ignition (radical explosion and thermal runaway) in hydrogen-air turbulent mixing layer at elevated pressure (1, 10, 30, 50 atm). Song et al. [29,30] provided the two and three-dimensional DNS on auto-ignition characteristics of the turbulent supercritical hydrothermal flame and found that there was no well-defined most reactive mixture fraction under supercritical conditions. Apart from hydrogen research in the mixing layer of auto-ignition, hydrocarbon fuels including n-heptane, methane and DME were also simulated to investigate the auto-ignition features under turbulent conditions using DNS. Sreedhara et al. [31,32] studied the n-heptane auto-ignition characteristics under homogeneous and decaying turbulence, showing the ignition kernels originated at the local vortex cores. Gopalakrishnan et al. [33] investigated the effects of multicomponent diffusion on the auto-ignition of one-dimensional n-heptane mixing layer. Detailed mechanism and 10–40 bar pressure conditions were employed. They found that the Dufour effect would decrease the ignition delay time while the Soret effect would increase it. Løvås et al. [34] also studied the three-dimensional auto-ignition turbulent non-premixed flames of n-heptane with simple and complex chemistry, showing the richer values of the most reactive mixture fraction and ignition could appear at higher scalar dissipation locations in the NTC regime. Mukhopadhyay et al. [35,36] revealed the effects of compositional stratification, heat release rate and turbulence on scalar dissipation rate in the auto-ignition mixing layer of n-heptane-air. They concluded that the heat release rate would affect the scalar dissipation rate by the balance between expansion of burned gases and increased laminar diffusivity due to combustion. Krisman et al. [37] studied the two-stage auto-ignition and edge flames features under 40 atm for n-heptane with global mechanism. They observed the quick growth of ignited kernels into edge flames which evolved along the stoichiometric mixture fraction iso-line. Oijen [38] calculated the one-dimensional methane-hydrogen mixing layer to investigate the auto-ignition features under laminar condition with MILD combustion and found that hydrogen chemistry was dominant in the ignition process and the effects of non-unity Lewis could not be neglected. DME was widely investigated in auto-ignition of mixing layer. Zhang et al. [39] illustrated the ignition process of DME in one-dimensional case with temperature inhomogeneities, combined with detailed chemistry at high pressure. Bansal et al. [40] have carried out three-dimensional DNS for the auto-ignition study of stratified DME/air mixtures and they have identified three stages of ignition. Pal et al. [41], Im et al. [42] and Pal et al. [43] have carried out DNS studies of auto-ignition characteristics of syngas under high pressure and low-temperature conditions for both laminar and turbulent flames with temperature inhomogeneity. They derived ignition regimes with respect to temperature fluctuations. Krisman et al. [44,45] investigated the two-dimensional mixing layer of DME using DNS under 40 atm, showing the clear two combustion regions (low temperature combustion and high temperature combustion). DME mixed with methane was also studied by Jin et al. [46] to exhibit the effects of cool flames and they found that auto-ignition kernels of high temperature were accelerated by the cool flame. Su et al. [47] conducted DNS study to investigate the DME/air mixture auto-ignition with different initial temperature distributions. They distinguished two combustion modes, including auto-ignition and flame propagation according to heat release rate contours, transport budget term and average temperature gradient.

As discussed above, many investigations were reported for the auto-ignition study of non-premixed flames for various fuels such as hydrogen, methane, n-heptane and DME in counterflow, jet flow and mixing layer configurations. However, the auto-ignition study of emerging fuels such as ammonia and ammonia-hydrogen fuel blends under engine relevant conditions such as high turbulence and elevated pressure are still lacking in the literature. So far, auto-ignition studies of ammonia and ammonia-hydrogen fuel blends were mainly focused on chemical mechanisms using zero-dimensional simulations or rapid compression machine for experiments [48–54]. Some combustion characteristics of ammonia and ammonia-hydrogen fuel blends were investigated in turbulent non-premixed combustion applications [55,56].

In the present study, the fundamental aspects of auto-ignition characteristics and subsequent flame development of ammonia-air and ammonia-hydrogen-air mixing layers under engine-relevant conditions are investigated by means of DNS with detailed chemical mechanism. All simulations were performed based on the mixing layer configuration with temperature stratification (standard fuel temperature and heated air temperature). We study the novel features of auto-ignition and flame evolution of ammonia and ammonia-hydrogen mixing layers for laminar and turbulent conditions under high pressure. The results are analysed in terms of scalar dissipation rate, heat release rate, and radical species concentrations. The remaining sections will discuss numerical methodology and initial conditions, results and discussion, and summary of key conclusions.

Numerical methodology and initial conditions for DNS

The auto-ignition and subsequent flame development of ammonia and ammonia-hydrogen mixing layers at elevated pressures are studied using the parallel DNS code, PARCOMB [57]. The DNS code solved the fully compressible Naiver-Stokes equations, consisting of the continuity, momentum, energy, transport for each species and the ideal gas equation on a uniform two-dimensional Cartesian grid. The transport equations for each species are simulated by applying the mixture-averaged transport model without the Soret effect and the radiation heat loss. Sixth-order central differencing scheme is applied to calculate the spatial derivatives and the

Please cite this article as: Yang W et al., Direct numerical simulations of auto-igniting mixing layers in ammonia and ammonia-hydrogen combustion under engine-relevant conditions, International Journal of Hydrogen Energy, https://doi.org/10.1016/j.ijhydene.2022.08.290

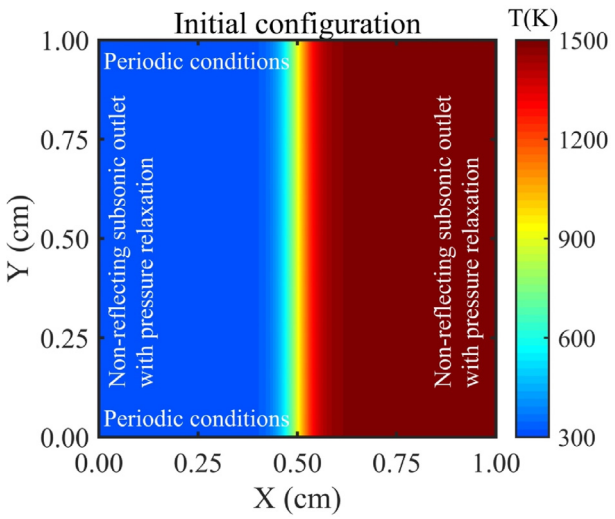

Fig. 1 – Initial temperature contour with boundary conditions.

order is progressively reduced to four at boundaries. The time integration is performed using the fourth-order Runge-Kutta scheme. To enhance the stability of iterations, the Courant-Friedrichs-Levy (CFL) condition for the convective term and the Fourier condition for the diffusion term are employed, resulting in a suitable time step. The Naiver-Stokes characteristics boundary conditions (NSCBC) with modified pressure relaxation [58] are used to keep the constant pressure on the left and right side of the two-dimensional computational domain. The periodic condition is implemented on the top and bottom boundaries of the two-dimensional computational domain. Random noise diffusion method [59] combined with the digital filtering is employed to generate the initial homogeneous isotropic turbulent velocity field. To keep the same turbulent Reynolds number at two different elevated pressures, two different turbulent intensities and integral length scales are applied. More detailed information and the validation of PARCOMB code can be found in Refs. [60,61], and the code has been extensively used to study different turbulent combustion problems including combustion characteristics at high turbulence and elevated pressure [27,28,62–65].

The mixing layer configuration as reported in Refs. [20,24,27,28] with temperature stratification under high turbulence intensity and elevated pressure is implemented (see Fig. 1). In two-dimensional computational domain, four turbulent mixing layer cases of DNS are designed for pure ammonia and ammonia-hydrogen fuel blends with standard fuel temperature of 300 K and heated air temperature of 1500 K. The four turbulent test cases are set for pure ammonia and ammonia-hydrogen fuel blends (90%–10% by volume) at two different elevated pressures of 10 atm and 20 atm, respectively. Table 1 shows detailed turbulent parameters and resolution of the computational domain for simulated cases. One-dimensional laminar mixing layer cases with the same fuels, grid resolution, and time step as the turbulent cases are also simulated under 10 atm and 20 atm, respectively. In addition, zero-dimensional simulations are also performed at same conditions. More details about the zero-dimensional cases will be discussed in the next section.

Table 1 – Initial pressure, turbulence conditions and grid resolution parameters for all four simulations.

Case number	Fuel	Pressure (atm)	u' (m/s)	l_t (mm)	Re_t[a]	Grid	Cell width (μm)	η(μm)[b]
Case 1	100% NH_3	10	0.4438	0.50	148	2001^2	5.0	11.78
Case 2	100% NH_3	20	0.4438	0.25	148	4001^2	2.5	5.89
Case 3	90% NH_3 10% H_2	10	0.4798	0.50	148	2001^2	5.0	11.78
Case 4	90% NH_3 10% H_2	20	0.4798	0.25	148	4001^2	2.5	5.89

u'-Root-mean-square (RMS) turbulent fluctuation velocity.
l_t-Integral length scale measured directly from the initial turbulence field.
[a] -Turbulent Reynolds number, $Re_t = u'l_t/\nu$.
[b] -Kolmogorov length scale, $\eta = l_t Re_t^{-0.75}$.

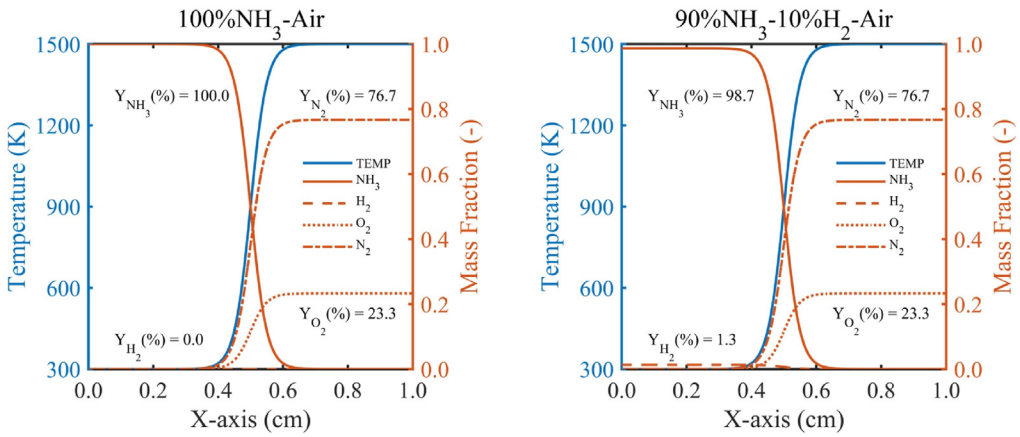

Fig. 2 – The initial profiles of temperature and radical species.

Please cite this article as: Yang W et al., Direct numerical simulations of auto-igniting mixing layers in ammonia and ammonia-hydrogen combustion under engine-relevant conditions, International Journal of Hydrogen Energy, https://doi.org/10.1016/j.ijhydene.2022.08.290

In this study, a detailed chemistry mechanism with 22 species and 66 elementary reactions proposed by Rocha et al. [48] is employed. The computational domain is 1 cm^2 for all four two-dimensional turbulent mixing layer cases, with two different uniform Cartesian grid points (2001^2 for 10 atm and 4001^2 for 20 atm), the grid resolution being 5.0 μm and 2.5 μm, for cases with 10 atm and 20 atm, respectively. The one-dimensional laminar mixing layer simulations are also calculated with the domain size of 1 cm. The CFL number is about 0.3, utilising to control the time step around 3 ns for 10 atm and 1.5 ns for 20 atm, respectively. This time step is appropriate compared to Ref. [66] with grid resolution of 20 μm and time step 5 ns under 0.1 MPa and reference [65] with 4.5 ns and 8 μm under 0.54 MPa. Meanwhile, the resolution in this study is between two and three times smaller than the Kolmogorov scale under 10 atm and 20 atm pressure conditions, which is fully required to resolve the smallest scale in the turbulent mixing layer auto-ignition scenarios. All simulations including four two-dimensional turbulent mixing layer cases were performed on ARCHER2 with 50 nodes (128 cores per node). The wall clock time for turbulent cases is about 255 h, equivalent to 1.62 million CPU hours. Fig. 1 illustrates the initially mixing layer configuration, which consists of fuel with standard temperature (100% NH_3 or 90% NH_3 blended with 10% H_2 at 300 K on the left hand side) and hot air (21% O_2 and 79% N_2 at 1500 K on the right hand side) by volume.

The initial profiles temperature and mass fractions of all species are described as:

$$\varphi = \varphi_0 + \frac{\Delta\varphi}{2}[1 - tanh(s \cdot (x - x_m))] \quad (1)$$

where $\Delta\varphi$ represents the difference of parameters between the cold fuel and hot air, including the temperature and mass fractions of all species. The x_m is the middle value of the x axis. The stiffness symbol of s evaluates the stratification in the mixing layer, which is equal to 2000 in the present study and same as references [27,28]. Fig. 2 shows detailed distribution of initial temperature and species mass fractions. Pure ammonia and ammonia-hydrogen fuel blends are simulated to compared the effects of hydrogen addition on the auto-ignition of ammonia combustion. In the non-premixed flame, the parameter of mixture fraction Z commonly describes the level of mixing in the reactants [67], 0 in the oxidizer side and 1 in the fuel side. In the present study, the mixture fraction considers all three elements of H, N, and O,

$$Z = \frac{0.25(Y_H - Y_{H,ox})/W_H + 0.75(Y_N - Y_{N,ox})/W_N - (Y_O - Y_{O,ox})/W_O}{0.25(Y_{H,fu} - Y_{H,ox})/W_H + 0.75(Y_{N,fu} - Y_{N,ox})/W_N - (Y_{O,fu} - Y_{O,ox})/W_O} \quad (2)$$

which is calculated using the following equation:
where Y_H, Y_N and Y_O are the element mass fractions of elements H, N, and O. The subscripts fu and ox represent the initial conditions on the fresh fuel and oxidizer sides, respectively. The mole weights of elements are written in W_H, W_N and W_O. Also, the scalar dissipation rate, χ, is calculated to evaluate the level of local mixing in the computation domain by including the thermal diffusivity D:

$$\chi = 2D(|\nabla Z|)^2 \quad (3)$$

Results and discussion

In this section we discuss auto-ignition characteristics based on zero-dimensional homogeneous mixing layer ignition (HMI), one-dimensional laminar flow mixing layer ignition (LMI), and two-dimensional turbulent flow mixing layer ignition (TMI), respectively. Although there are different definitions [24] to calculate the auto-ignition delay time based on temperature, heat release rate, and some specific radicals, difference among these calculation results seems negligible. In the present study, the auto-ignition delay time t_{ign} is defined by the maximum heat release rate H_{max} using the following equation:

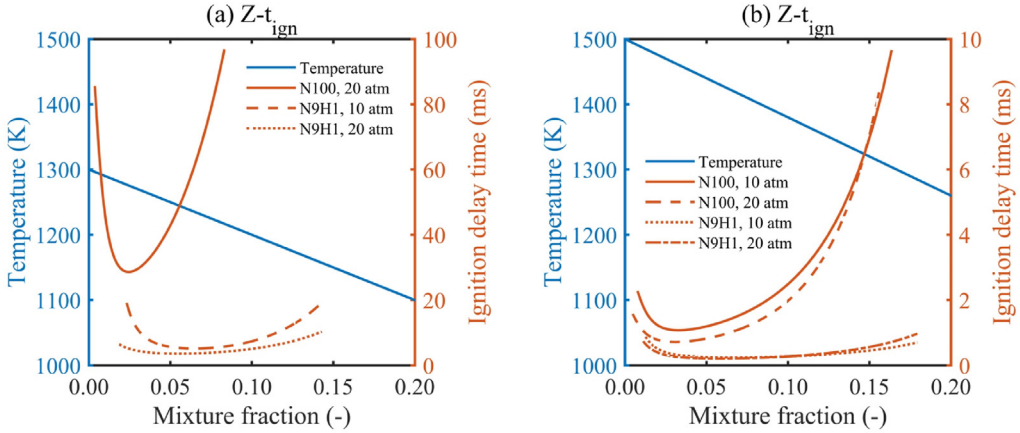

Fig. 3 – Zero-dimensional auto-ignition delay time along mxiture fraction.

Please cite this article as: Yang W et al., Direct numerical simulations of auto-igniting mixing layers in ammonia and ammonia-hydrogen combustion under engine-relevant conditions, International Journal of Hydrogen Energy, https://doi.org/10.1016/j.ijhydene.2022.08.290

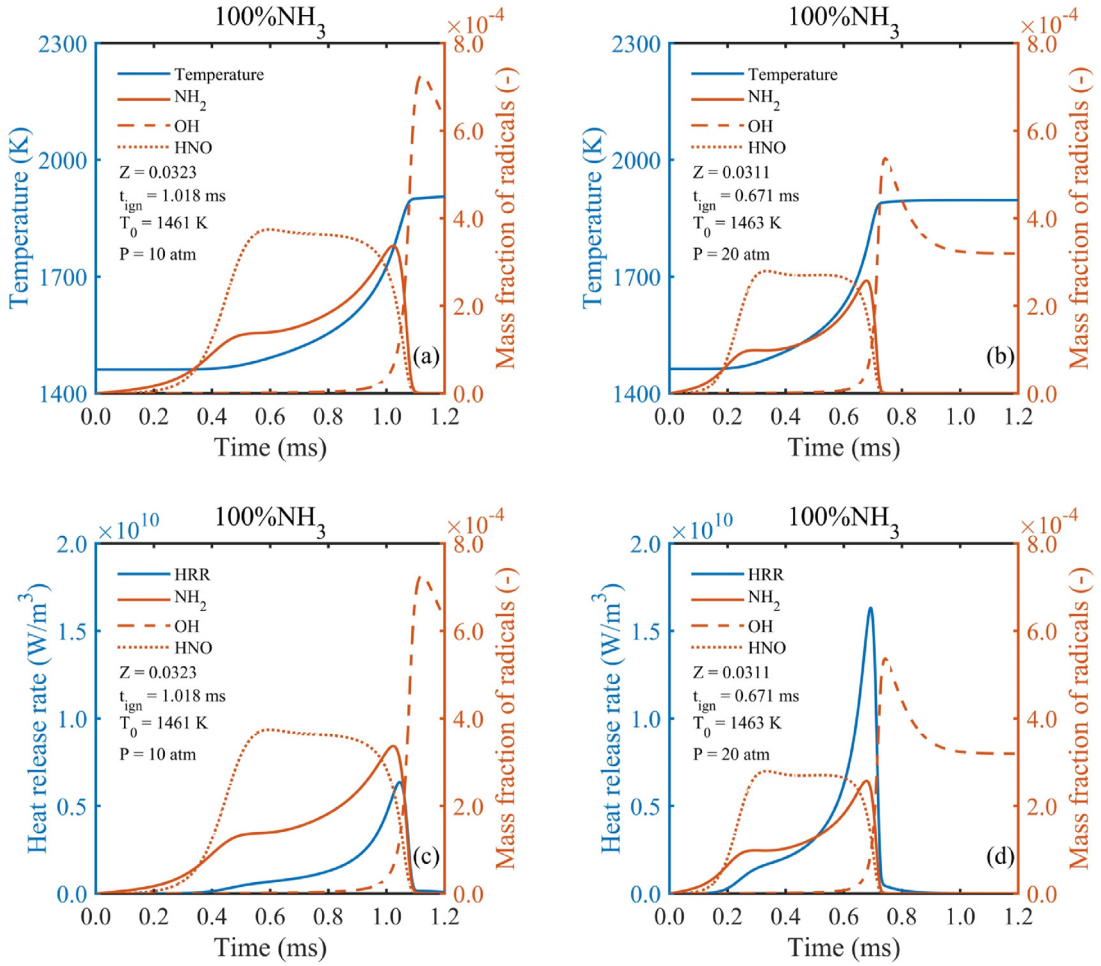

Fig. 4 – Auto-ignition process under most reactive mixture fraction obtained from zero-dimensional calculation for 100% NH_3 at 10 atm and 20 atm.

$$\frac{\partial^2 H_{max}}{\partial t^2}|_{t=t_{ign}} = 0 \tag{4}$$

Zero-dimensional flame simulations

In this study, we performed zero-dimensional flame simulations only to study the effects of chemistry on the auto-ignition without taking diffusion and convection into account. According to Ref. [3], the auto-ignition occurs along the most reactive mixture fraction Z_{mr} iso-line, which can be pre-computed by a series of homogeneous reactor based on different initial temperature and mass fractions. After the calculation of mixture fraction, the computation domain is reconstructed. The mass fractions of all four species (NH_3, H_2, O_2, N_2) and temperature can be expressed linearly as the function of mixture fraction:

$$\begin{aligned} Y_{NH_3} &= Y_{NH_3,fu}Z, \\ Y_{H_2} &= Y_{H_2,fu}Z, \\ Y_{O_2} &= Y_{O_2,ox}(1-Z), \\ Y_{N_2} &= Y_{N_2,ox}(1-Z), \\ T &= T_{ox} - Z(T_{ox} - T_{fu}). \end{aligned} \tag{5}$$

where $Y_{NH_3} = 1$, $Y_{H_2} = 0$ for pure ammonia-air mixing or $Y_{NH_3} = 0.987$, $Y_{H_2} = 0.013$ for ammonia-hydrogen-air mixing. The mass fractions of the hot oxidizer are the same for both two fuels, $Y_{O_2} = 0.233$, $Y_{N_2} = 0.767$. Considering the difficulty of ignition of pure ammonia, the temperature of air is slightly high with $T_{ox} = 1500\ K\ and\ T_{fu} = 300\ K$. Another temperature profile with $T_{ox} = 1300\ K$ is simulated in HMI as comparison. All zero-dimensional cases are simulated in Cantera [68] with 0.1 ms time step until combustion is achieved.

Fig. 3 (a) and (b) show the auto-ignition delay time of a series of homogeneous mixing ignition points and two different initial temperature profiles of 1300 K and 1500 K as a function of the mixture fraction for NH_3 and NH_3–H_2 cases at 10 atm ad 20 atm, respectively. At the very lean mixture condition, the initial temperature is high while at the very rich mixture condition, the initial temperature is low. Hence, the curve of auto-ignition delay time corresponding with the mixture fraction shows the minimum ignition time and the most reactive mixture fraction Z_{mr} where this minimum value appears. We find that it takes a much longer time to ignite with a lower initial temperature of 1300 K in Fig. 3 (a), which indicates that DNS of the laminar and turbulent mixing layer with 1300 K on the oxidizer side would require much computational cost to

Please cite this article as: Yang W et al., Direct numerical simulations of auto-igniting mixing layers in ammonia and ammonia-hydrogen combustion under engine-relevant conditions, International Journal of Hydrogen Energy, https://doi.org/10.1016/j.ijhydene.2022.08.290

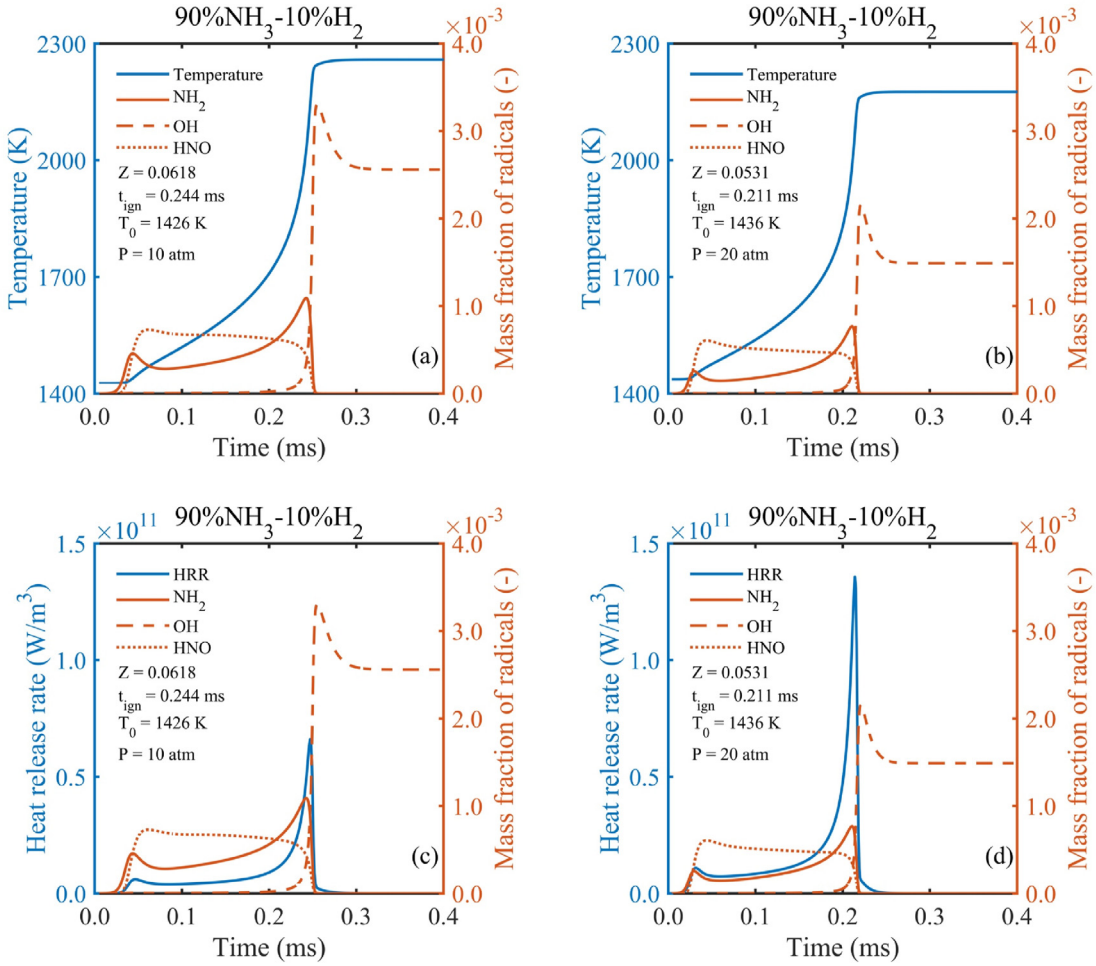

Fig. 5 – Auto-ignition process under most reactive mixture fraction obtained from zero-dimensional calculation for 90% NH_3 – 10% H_2 at 10atm and 20 atm.

reach the same scale of ignition delay time, especially for pure ammonia-air cases at 10 atm and 20 atm, respectively. The ignition delay time of HMI in Fig. 3 (b) with oxidizer temperature of 1500 K is lower than 10 ms for all four test cases, which might be further reduced in turbulent mixing field. This will cause the auto-ignition and flame development with acceptable DNS computational cost. Therefore, we used the oxidizer temperature of 1500 K for the DNS test cases. Based on the oxidizer temperature of 1500 K, the most reactive mixture fraction values are 0.0323, 0.0311, 0.0618, 0.0531 for NH_3 and NH_3–H_2 at 10 atm and 20 atm, respectively, which are much leaner compared with pure hydrogen-air mixing layer in Refs. [27,28]. The results also show that increasing pressure reduces the most reactive mixture fraction, while hydrogen addition into ammonia increases this value. These four most reactive mixture fraction values (Z_{mr}) are applied to analyse one-dimensional laminar and two-dimensional turbulent mixing layer simulation results.

Figs. 4 and 5 show temperature, heat release rate and mass fractions of three selected radicals (NH_2, OH, HNO) as a function of time for NH_3 and NH_3–H_2 fuel blends at the most reactive mixture fraction location, respectively. The results indicate that even 10% hydrogen addition by volume greatly increases the final temperature value. The hydrogen addition and elevated pressure both have a noticeable effect on ignition delay time as they both reduce ignition delay time independently. The high-pressure condition results in higher peak of heat release rate while relatively lower final temperature. This is because the mixture fraction is higher, which means more fuel at low pressure conditions. The temperature curves in Fig. 4 (a), (b) and Fig. 5 (a), (b) display one temperature increment stage while the heat release rate in Fig. 4 (c), (d) and Fig. 5 (c), (d) shows two peaks, which are more distinct for ammonia blended with hydrogen compared to pure ammonia. Here, the first peak of heat release rate corresponds to the increment of appearance in temperature (induction stage due to increase of heat release rate with accumulation of radicals) and the second peak of heat release rate corresponds to the steady maximum temperature regime (thermal runaway stage where heat release rate becomes zero).

The previous studies found that pure hydrogen in HMI [27,28] exhibits accumulation of radicals only in the induction stage including radical OH, where temperature rise occurred. However, our current study finds different trends for ammonia and ammonia-hydrogen cases compared to pure hydrogen in HMI. For example, our results show that radical OH is keeping nearly nothing and undergoes a sudden increment until temperature reaches its maximum value. The

Please cite this article as: Yang W et al., Direct numerical simulations of auto-igniting mixing layers in ammonia and ammonia-hydrogen combustion under engine-relevant conditions, International Journal of Hydrogen Energy, https://doi.org/10.1016/j.ijhydene.2022.08.290

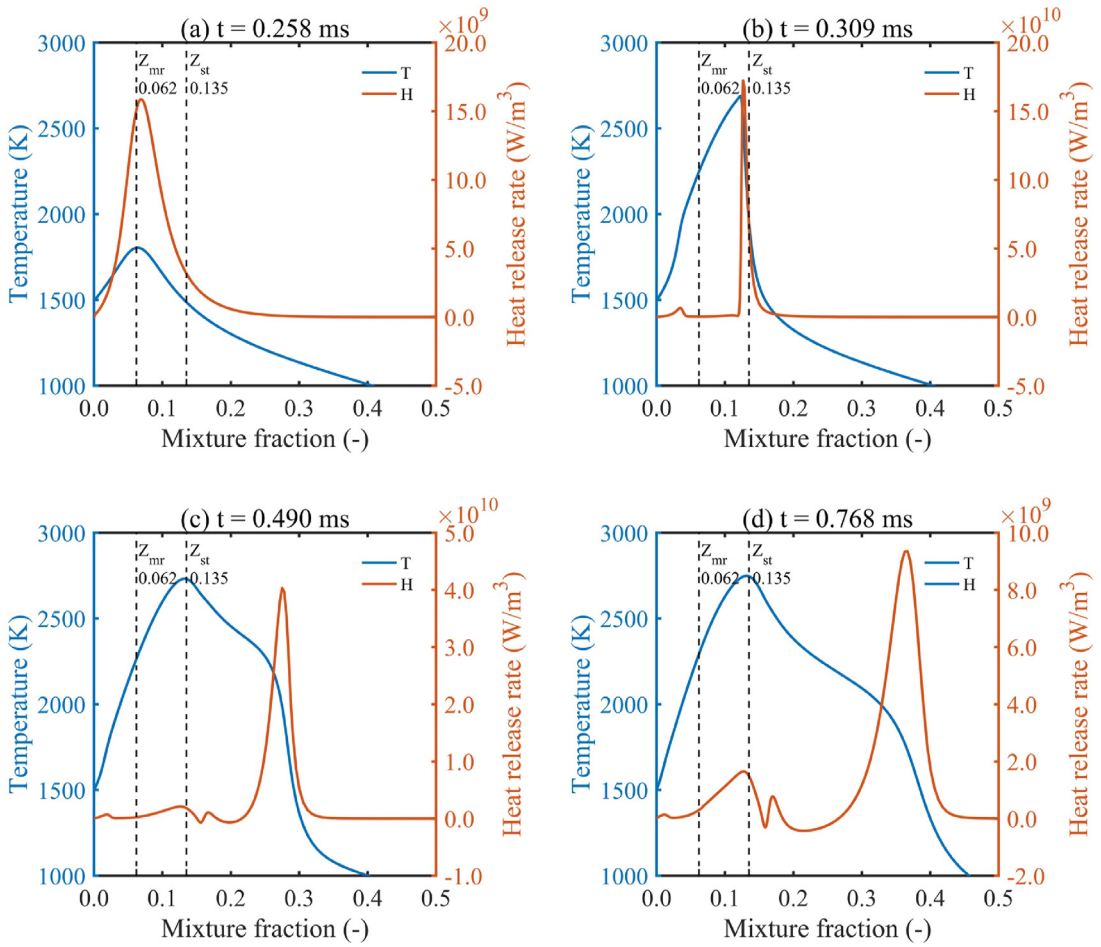

Fig. 6 – Auto-ignition process of 90% NH_3 – 10% H_2 in one-dimensional laminar flame calculations (Temperature and HRR at 10 atm).

radical OH is partially reduced and reaches a stable value at the thermal runaway stage. The results also show that unlike OH, NH_2 and HNO only appear in the induction stage. The radical NH_2 continue to grow at the induction stage and then quickly goes down to zero value. The distribution of radical NH_2 is almost same as the heat release rate evolvement for NH_3 and NH_3–H_2 mixture, which indicates that the radical NH_2 can be regarded as a potential heat release rate marker just like in Ref. [65]. The radical HNO achieves the maximum value at the early induction stage, then slightly reduces at the whole induction stage, and finally becomes zero like the NH_2 radical. The findings indicate that hydrogen addition increases all values of all three radicals and HMI under elevated pressure shows relatively low level of radicals, the reason of which is the same as that for lower final temperature cases. These three specific radicals clearly distinguish the HMI auto-ignition process, marking the low and high temperature, and heat release rate regimes, potentially useful for the analysis of one and two-dimensional mixing layers.

One-dimensional laminar flame simulations

The intention of this section is to elucidate valuable information about the auto-ignition characteristics of NH_3 and NH_3–H_2 fuels at elevated pressure based on the scalar dissipation rate computed via the thermal diffusivity and the gradient of the mixture fraction. Four cases of one-dimensional laminar flame simulations for NH_3 and NH_3–H_2 at 10 atm and 20 atm are simulated (see simulated test cases in Table 1). Compared with zero-dimensional homogenous cases, diffusion effects are employed in one-dimensional laminar mixing layers.

Fig. 6 and Fig. 7 illustrate the distribution of temperature, heat release rate, scalar dissipation rate, and three selected radicals found from the previous homogeneous study along the whole mixture fraction domain at four-time instants for NH_3–H_2 fuel blends at 10 atm. Two dashed lines are plotted, representing the most reactive mixture fraction and the stoichiometric mixture fractions, respectively. Since we found similar observations in other cases, we only present results for the one test case. The plots for other cases are presented in the supplementary document.

When the auto-ignition happens at 0.258 ms, the two peaks of temperature and heat release rate rise, centred nearly at the most reactive mixture fraction location. As the heat release marker, NH_2 radical shows almost the same profile as the heat release rate. The major contribution to the overall heat release rate around the ignition location is related to the elementary

Please cite this article as: Yang W et al., Direct numerical simulations of auto-igniting mixing layers in ammonia and ammonia-hydrogen combustion under engine-relevant conditions, International Journal of Hydrogen Energy, https://doi.org/10.1016/j.ijhydene.2022.08.290

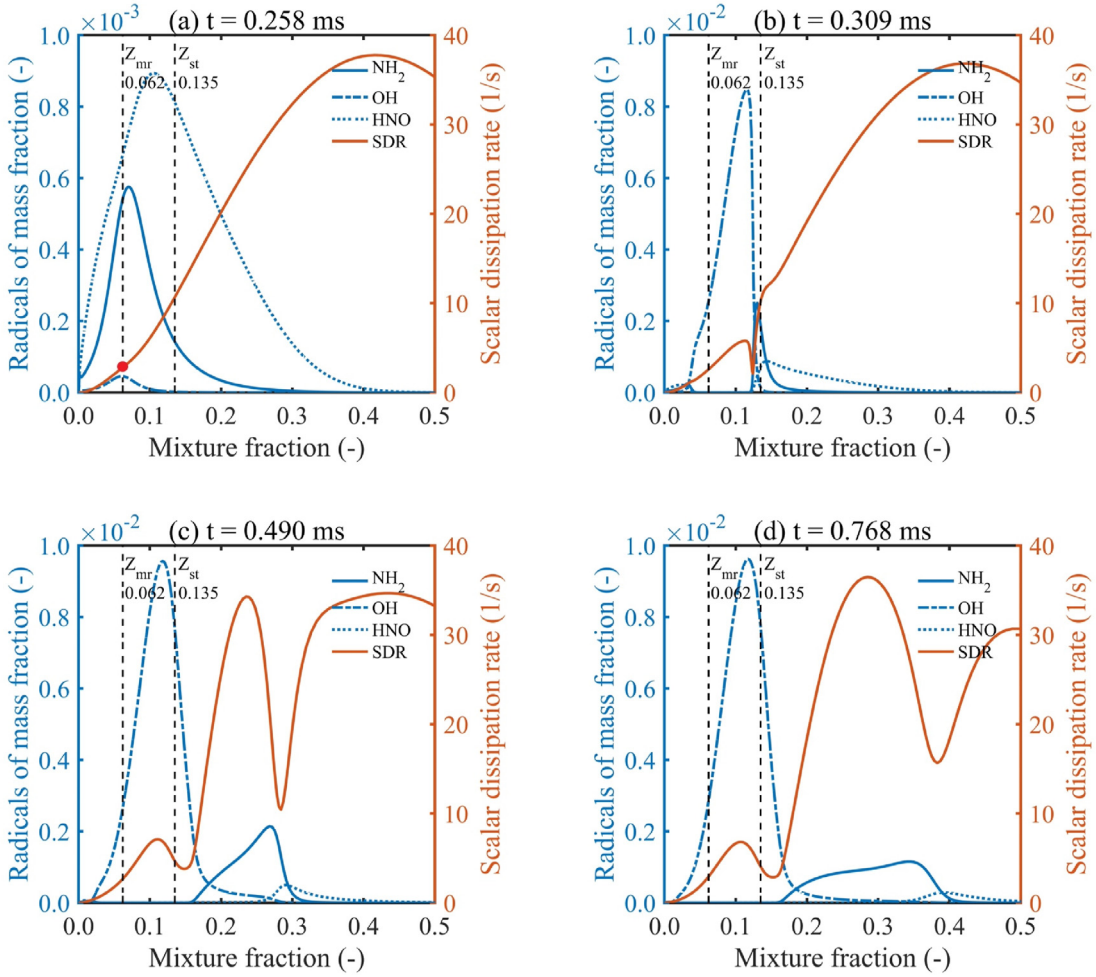

Fig. 7 – Auto-ignition process of 90% NH_3 – 10% H_2 in one-dimensional laminar flame calculations (SDR and radicals at 10 atm).

reactions including radical NH_2, which can be seen in the elementary reaction diagram in supplementary document. We observe a wider distribution of HNO and nearly nothing of OH due to the relatively low temperature value along the whole domain at this initial auto-ignition moment, also called the induction stage. After that the temperature profile increases more rapidly on the lean side and propagates towards the stoichiometric mixture fraction site accompanied by an increase of heat release rate at 0.309 ms. There is a lower region of scalar dissipation rate where exactly the peak of heat release rate locates. At this moment, OH reaches the maximum value and no NH_2 and HNO are observed, which indicate disappearance of the induction stage and the dominant role of the thermal runaway stage on the lean side. When the peak value of heat release rate passes through the stoichiometric mixture fraction location, the maximum temperature is located at the Z_{st} line and temperature and OH profiles on the lean side keeps almost identical. The rise of temperature in the fuel rich side is continuously driven by the peak of heat release rate, while its value is relatively lower at 0.490 ms compared with that at 0.309 ms. The NH_2 region becomes a little wider while keeping its peak value same as the peak value of heat release rate. Meanwhile, HNO only exists in the lower temperature region where the mixture fraction is more than 0.3. At 0.768 ms, two local maximum values of heat release rate are observed, the first one at the Z_{st} location and the second one still moving towards more fuel-rich side while NH_2 region changes broadly and its peak value coincides with the second peak of heat release rate. Meanwhile, two local minimum values of scalar dissipation rate appear around two peak values of heat release rate. However, the profile of OH is almost same as the previous time instant, where the maximum value is located between Z_{mr} and Z_{st}. There is a region where temperature values are almost the same in lean ($Z = 0.062$) and rich sides ($Z = 0.2$), we still observe a little OH and NH_2 radicals in the rich side, which indicates it is the boundary between the induction stage and the thermal runaway stage based on previous results from HMI cases. The first peak of heat release rate near the Z_{mr} iso-line should be mainly related with elementary reactions of OH because no NH_2 and HNO are distributed at this location. This peak is utilised to maintain the highest temperature at the Z_{st} location while the second peak of heat release rate is raising the temperature of the entire fuel-rich area. At the later stage of auto-ignition of ammonia fuel, the phenomena of two local maximum values of heat release rate, which can also be called

Please cite this article as: Yang W et al., Direct numerical simulations of auto-igniting mixing layers in ammonia and ammonia-hydrogen combustion under engine-relevant conditions, International Journal of Hydrogen Energy, https://doi.org/10.1016/j.ijhydene.2022.08.290

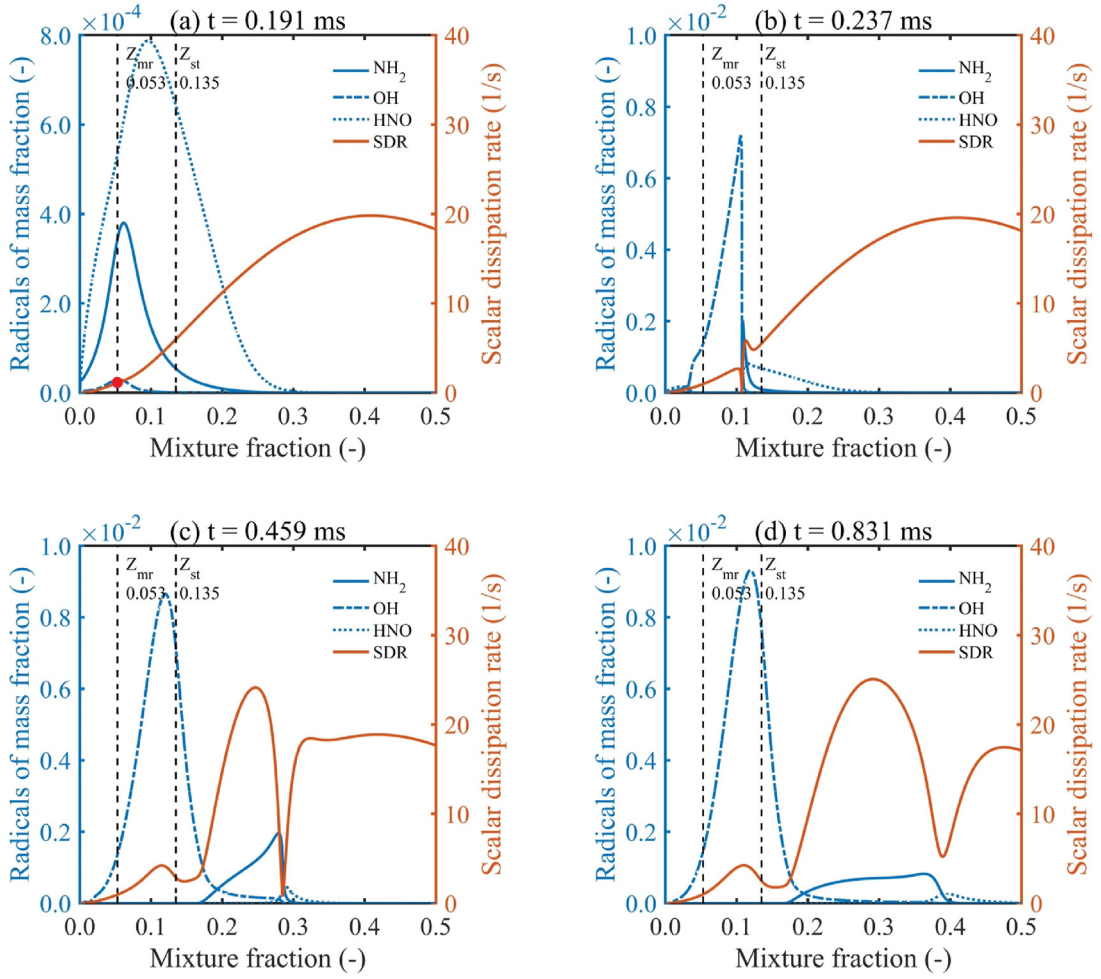

Fig. 8 – Auto-ignition process of 90% NH_3 – 10% H_2 in one-dimensional laminar flame calculations (SDR and radicals at 20 atm).

Table 2 – The scalar dissipation rate at the auto-ignition location for 1D laminar cases.

Case of Laminar	Pressure (atm)	Scalar dissipation rate (1/s)
100% NH_3	10	0.6875
100% NH_3	20	0.3516
90% NH_3 10% H_2	10	2.8178
90% NH_3 10% H_2	20	1.0846

heat release rate stratification, are also observed in two-dimensional turbulent mixing layer simulations.

To evaluate the pressure effects on the scalar dissipation rate, we then plot several parameters (same parameters as in Fig. 7) in Fig. 8 for 90% NH_3 – 10% H_2 fuel blends at 20 atm. The results show that the auto-ignition at 20 atm (0.191 ms) happens faster than that of at 10 atm (0.258 ms). The overall process is under much lower scalar dissipation rate, showing the heat release rate propagation corresponding with almost zero value of scalar dissipation rate at 0.237 ms and 0.459 ms. For all four one-dimensional laminar cases, the specific values of scalar dissipation rate at the ignition point can be derived by the crossing point, the red dot in Figs. 7 (a) and Fig. 8 (a), between the most reactive mixture fraction line and the scalar dissipation rate line, showing in Table 2 for all four simulated laminar test cases. The comparison between 10 atm and 20 atm in Figs. 7 and 8 shows that elevated pressure not only reduces the scalar dissipation rate at the ignition point, but also the rate in downstream of the flame development according to the scalar dissipation rate evolvement. The results between NH_3 and NH_3–H_2 test cases show that hydrogen addition in laminar mixing layers increases the scalar dissipation rate under the same pressure due to its high diffusivity, and speeds up the ignition because of the higher reactivity of hydrogen in the NH_3–H_2 fuel blends compared to pure NH_3 fuel. The relevant plots for two pure NH_3-air laminar mixing layer test cases at 10 atm and 20 atm are available in the supplementary document. In general, the effects of elevated pressure and hydrogen addition into ammonia on the scalar dissipation rate are just opposite over the entire mixture fraction region for simulated one-dimensional laminar mixing layer cases.

Please cite this article as: Yang W et al., Direct numerical simulations of auto-igniting mixing layers in ammonia and ammonia-hydrogen combustion under engine-relevant conditions, International Journal of Hydrogen Energy, https://doi.org/10.1016/j.ijhydene.2022.08.290

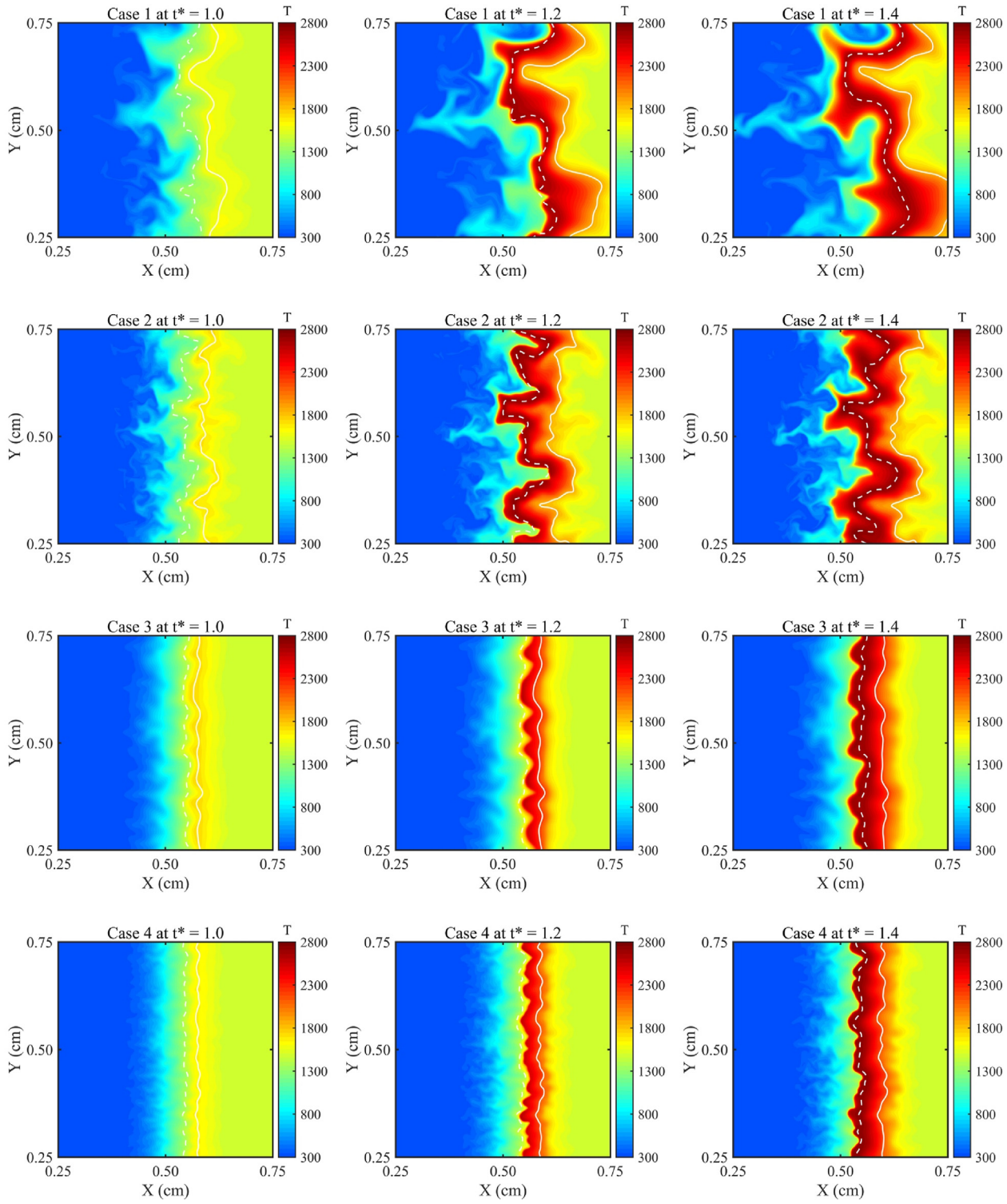

Fig. 9 – Contour plots of temperature obtained from two-dimensional turbulent flame simulations.

Two-dimensional turbulent flame simulations

In this section, we discuss results obtained from two-dimensional turbulent mixing layer simulations for pure NH_3 and NH_3–H_2 fuel blends at 10 atm and 20 atm respectively. The presence of turbulence creates highly wrinkled mixing layers with the development of auto-ignition and subsequent flame propagation. Figs. 9 and 10 show contour plots of temperature and scalar dissipation rate of two-dimensional turbulence mixing layers for all four cases at the same three non-dimensional time instants ($t^* = t/\tau_{tur} =$ 1.0, 1.2, 1.4). The actual physical values of the auto-ignition delay time τ_{tur} are provided in Table 3 in the next section. Two white iso-lines in each contour plot represent the most

Please cite this article as: Yang W et al., Direct numerical simulations of auto-igniting mixing layers in ammonia and ammonia-hydrogen combustion under engine-relevant conditions, International Journal of Hydrogen Energy, https://doi.org/10.1016/j.ijhydene.2022.08.290

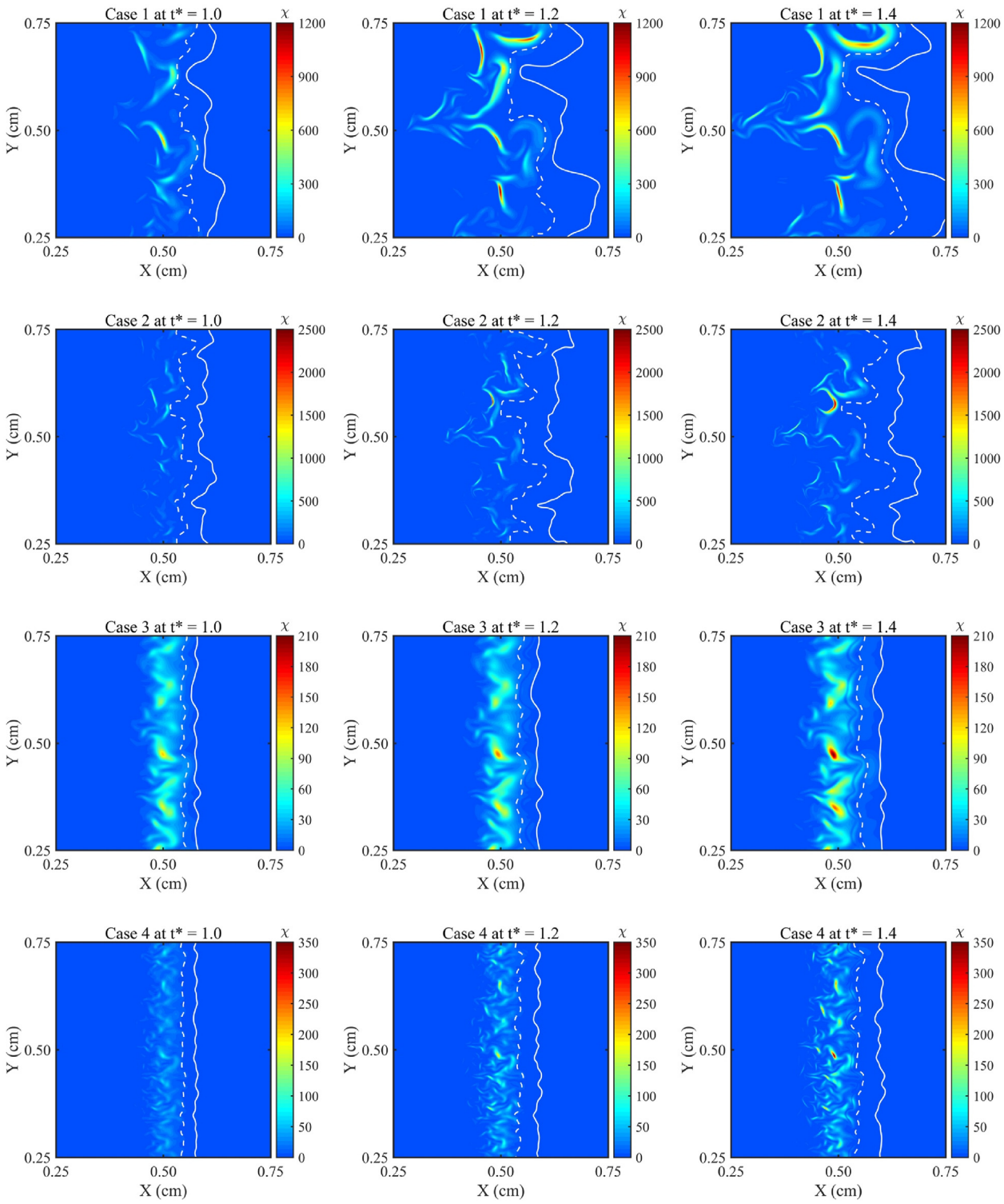

Fig. 10 – Contour plots of scalar dissipation rate obtained from two-dimensional turbulent flame simulations.

Table 3 – Auto-ignition delay times of one-dimensional laminar (τ_{la}), two-dimensional turbulent (τ_{tur}), and difference ($\Delta = \tau_{la} - \tau_{tur}$).

Case number	Fuel	Pressure (atm)	τ_{la} (ms)	τ_{tur} (ms)	Δ (ms)
Case 1	100% NH_3	10	1.278	1.209	0.069
Case 2	100% NH_3	20	0.792	0.695	0.097
Case 3	90% NH_3 10% H_2	10	0.258	0.247	0.011
Case 4	90% NH_3 10% H_2	20	0.194	0.191	0.003

Please cite this article as: Yang W et al., Direct numerical simulations of auto-igniting mixing layers in ammonia and ammonia-hydrogen combustion under engine-relevant conditions, International Journal of Hydrogen Energy, https://doi.org/10.1016/j.ijhydene.2022.08.290

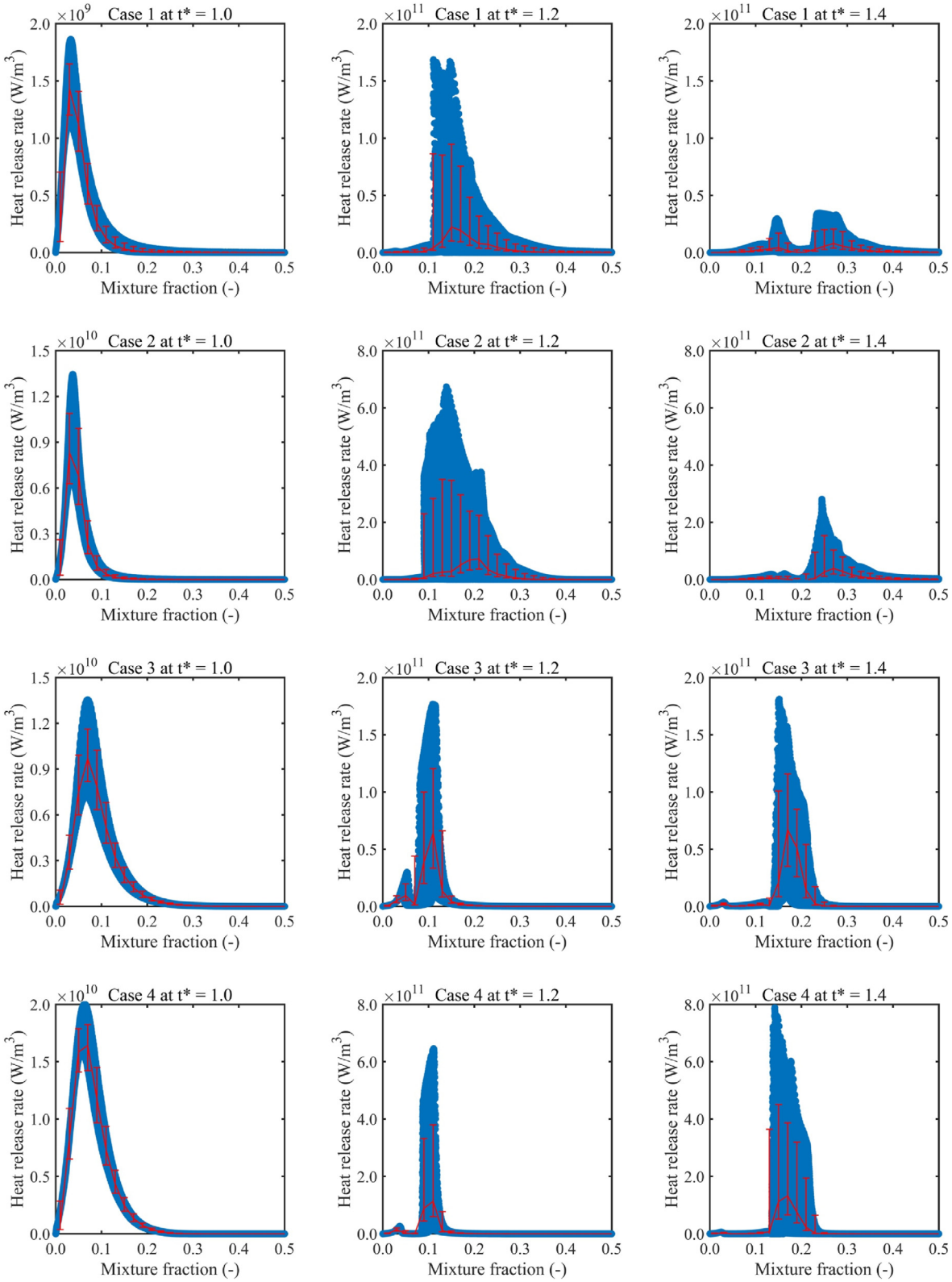

Fig. 11 – Scatter plots of heat release rate obtained from two-dimensional turbulent flame simulations.

reactive mixture fraction Z_{mr} (solid line) and stoichiometric mixture fraction Z_{st} (dashed line). The value of Z_{mr} is calculated from zero-dimensional cases, which successfully corresponds to the auto-ignition locations. Not all points along the most reactive mixture fraction iso-line show the auto-ignition kernels, which can be seen in separate locations in Fig. 10 with high temperature at ignition time instant ($t^* = 1.0$). The auto-ignition kernels are much clear in terms of heat

Please cite this article as: Yang W et al., Direct numerical simulations of auto-igniting mixing layers in ammonia and ammonia-hydrogen combustion under engine-relevant conditions, International Journal of Hydrogen Energy, https://doi.org/10.1016/j.ijhydene.2022.08.290

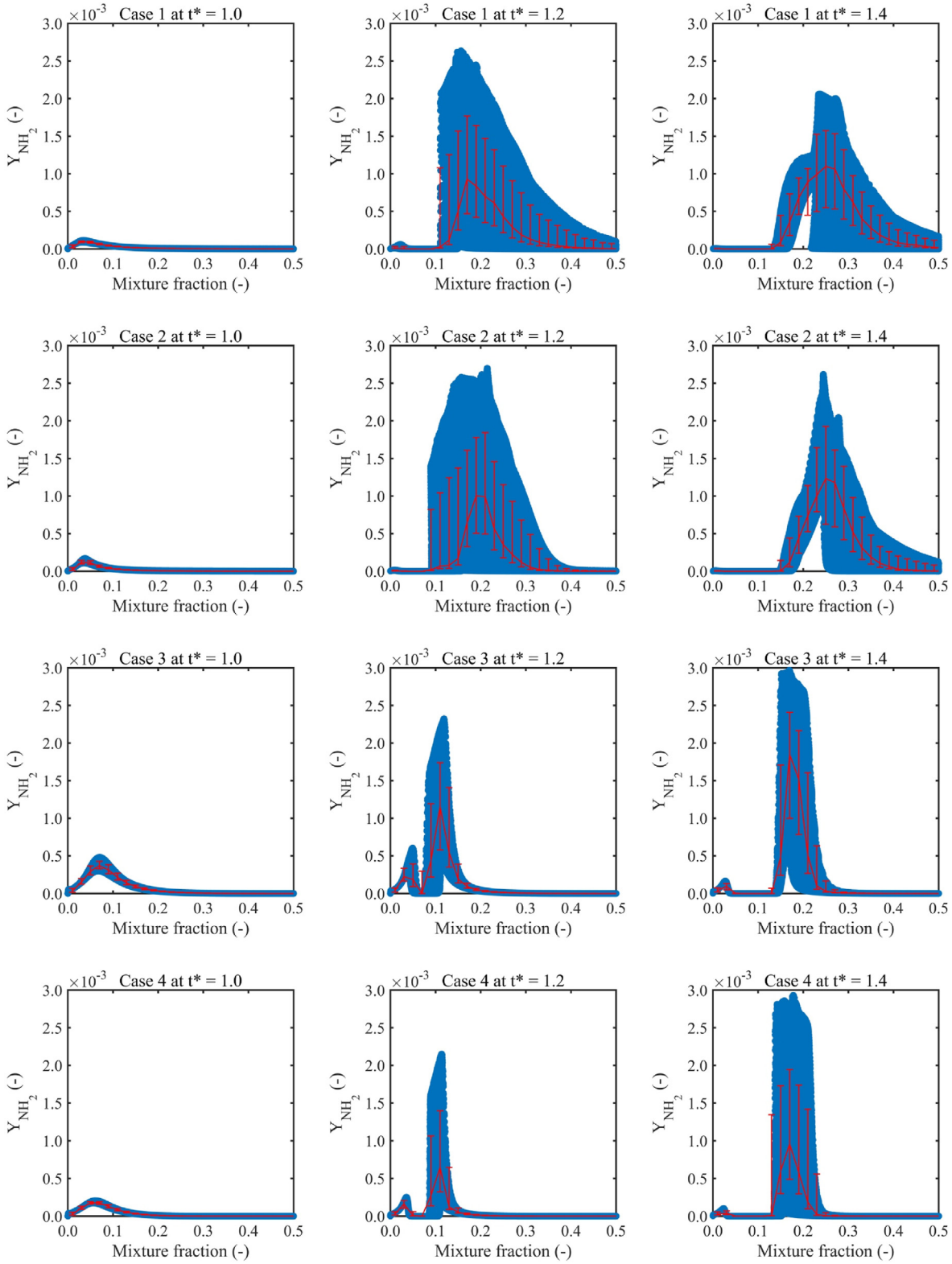

Fig. 12 – Scatter plots of radical NH_2 obtained from two-dimensional turbulent flame simulations.

release rate contour plots available in the supplementary document. It can be seen that after the auto-ignition, the high temperature region expands and propagates from the most reactive mixture fraction iso-line towards the stoichiometric mixture fraction iso-line ($t^* = 1.2$) and the highest temperature region stabilises along the stoichiometric mixture fraction iso-line ($t^* = 1.2$). It takes more physical time for ammonia-hydrogen-air mixing layers (Case 3 and 4) to

Please cite this article as: Yang W et al., Direct numerical simulations of auto-igniting mixing layers in ammonia and ammonia-hydrogen combustion under engine-relevant conditions, International Journal of Hydrogen Energy, https://doi.org/10.1016/j.ijhydene.2022.08.290

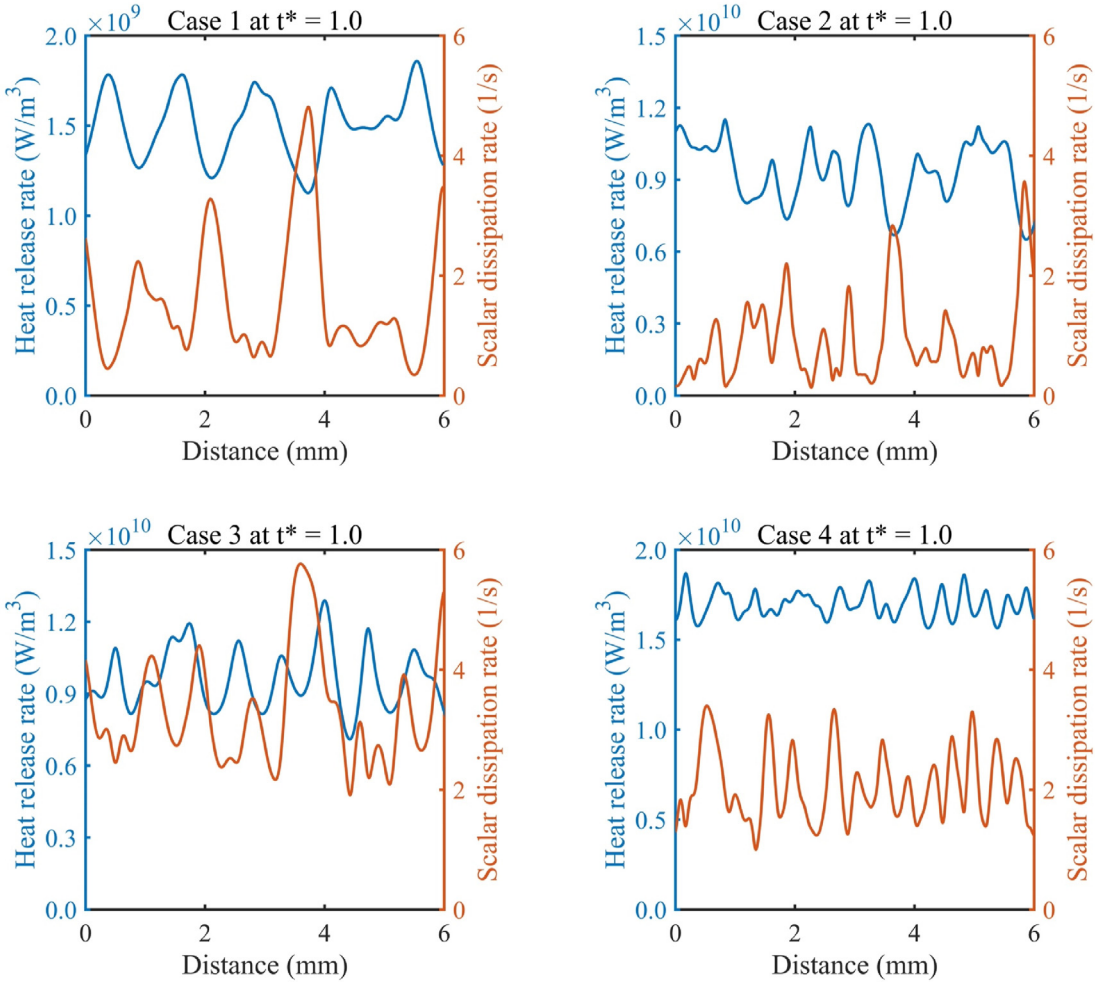

Fig. 13 – Heat release rate (left y-axis) versus the scalar dissipation (right y-axis) along the most reactive mixture iso-line obtained from two-dimensional turbulent flame simulations at the ignition time instant.

complete the process of propagation and stabilisation along the stoichiometric mixture fraction iso-line, although hydrogen accelerates the auto-ignition process. With the same turbulence level for the same fuel, elevated pressure obviously increases the number of auto-ignition kernels ($t^* = 1.0$), with more regions of high temperature and heat release rate. Meanwhile, combustion zones become thinner throughout the whole process. Turbulent mixing layers are fully wrinkled and wrinkling structures enhance the fuel and oxidizer mixing and eventually accelerate the auto-ignition process. The major distribution of the scalar dissipation rate is located at the downstream of combustion away from the most reactive mixture fraction iso-line and closer to the fuel-side. For the same fuel, increasing pressure causes more wrinkled structures, definitely leading to higher values of scalar dissipation rate on the fuel sides far from the most reactive mixture fraction, which is different for the same test case under laminar conditions. Similarly, the hydrogen addition has a negative influence on the scalar dissipation rate. Furthermore, less wrinkled structures are observed in the ammonia-hydrogen-air mixing layers compared with pure ammonia-air mixing layer cases under the same pressure. This might be due to high reactivity and faster burning rate of hydrogen fuel in the NH_3–H_2 fuel mixture via preferential diffusion effects [62,63]. However, further investigation is necessary to explicitly identify the role of preferential diffusion on the auto-ignition and subsequent flame development of NH_3–H_2 fuel blends compared to pure NH_3 under high turbulence and elevated pressure conditions.

Fig. 11 exhibits the scatter plots of heat release rate for all four turbulent cases. At the time ($t^* = 1.0$) of appearance of auto-ignition, only one peak of heat release rate arises at the locations of the most reactive mixture fraction in Fig. 11. The stratification of heat release rate is appeared for Case 1 at $t^* = 1.4$, observed in Fig. 11, and the heat release rate contour plot in the supplementary document. This finding is consistent with laminar flame results presented in the earlier section. Fig. 12 displays the scatter plots of radical NH_2. Radical NH_2 development further shows that it can be distinctly considered as the heat release rate marker under the comparison with Fig. 11. Meanwhile, two different regions are appeared for Case 1 at $t^* = 1.4$, the left side is narrow and the right side is wide. The

Please cite this article as: Yang W et al., Direct numerical simulations of auto-igniting mixing layers in ammonia and ammonia-hydrogen combustion under engine-relevant conditions, International Journal of Hydrogen Energy, https://doi.org/10.1016/j.ijhydene.2022.08.290

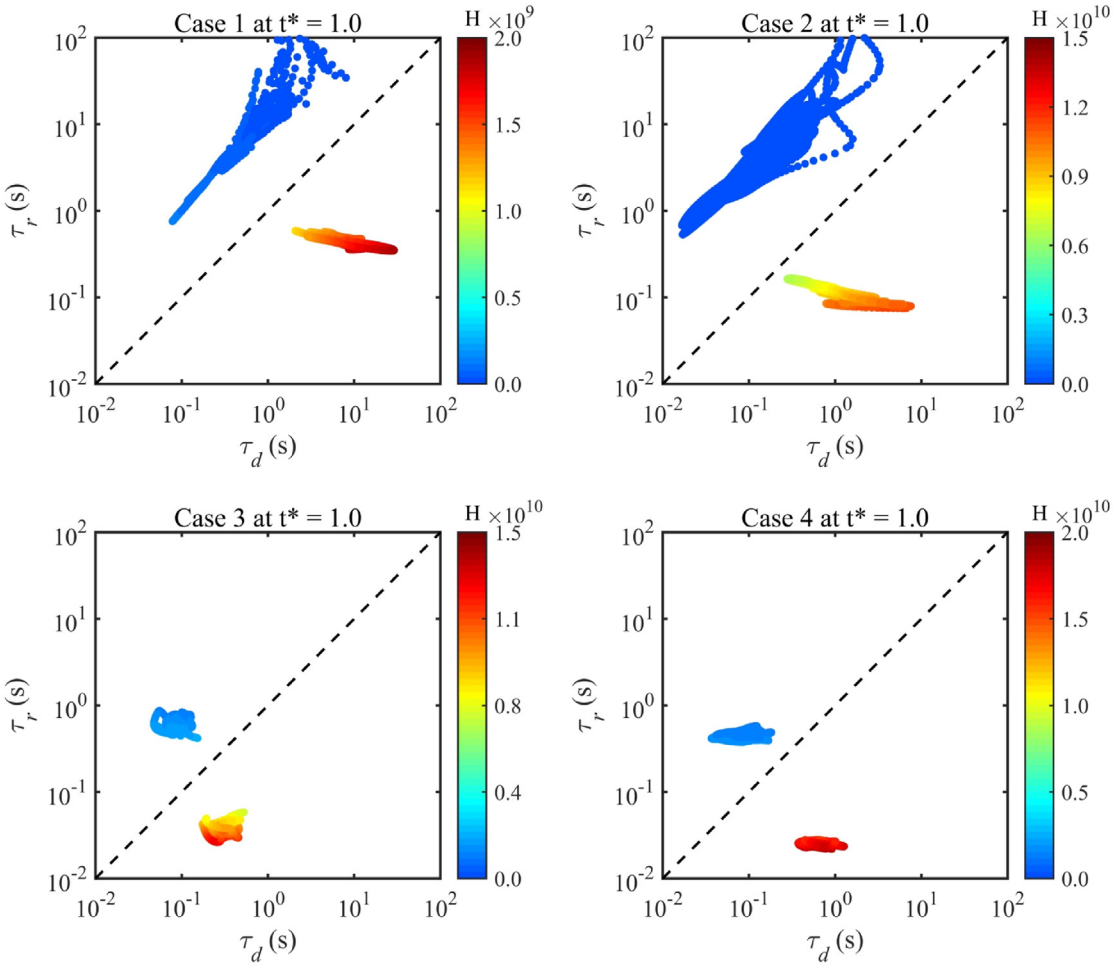

Fig. 14 – Diffusion time versus reaction time of radical NH_2 along the stoichiometric mixture fraction iso-line (the blue region) and the most reactive mixture fraction iso-line (the red region) obtained from turbulent flame simulations at the ignition time instant. (For interpretation of the references to color/colour in this figure legend, the reader is referred to the Web version of this article.)

borderline between these two different regions distinguishes the end (left side) and beginning (right side) of induction stage, which also represents the low temperature regions with the major scatter distribution of radical HNO. The scatter plots of radical species HNO and OH are included in the supplementary document. The overall trend of all three radicals in turbulent simulations is similar as the observation in zero and one-dimensional laminar cases. We hardly observe the radical OH until the reaction regions undergo the shift from auto-ignition towards fully combustion. The regions with stable temperature values are expanding with the continuous production of OH and finally the peak of this radical stabilises at the locations of the stoichiometric mixture fraction.

Due to the existence of turbulence, the range of scalar dissipation rate in Fig. 10 is too large in the whole computational domain. Hence, the specific values of the scalar dissipation rate and heat release rate are extracted along the most reactive mixture fraction iso-line for all four turbulent cases at the ignition time, and plotted in Fig. 13. The opposite distribution between these two parameters is obvious, illustrating that initial kernels are originating from locations with relatively lower scalar dissipation rate values. Meanwhile, the values of scalar dissipation rate at the ignition kernels in turbulent conditions are relatively close to the trends observed in one-dimensional laminar flames. Furthermore, the effects of elevated pressure and hydrogen addition on the scalar dissipation rate at the location of turbulent mixing layers are consistent with the tendency in laminar cases. However, the pressure and hydrogen addition show the opposite influence on the scalar dissipation rate for laminar and turbulent results in the downstream of the flame development.

Considering the importance of radical NH_2 in ammonia combustion, the time scale of diffusion ($\tau_d\,(s) = 1/\chi$) and reaction of NH_2 ($\tau_r\,(s) = \rho/\omega_{NH_2}$) are calculated using the same equations employed in Ref. [35], where χ is the scalar dissipation rate, ρ is the density, and ω_{NH_2} is the reaction rate in the computational domain. Fig. 14 compares these two-time scales of radical NH_2, two regions along the most reactive and stoichiometric mixture fraction iso-lines. The dashed line

Please cite this article as: Yang W et al., Direct numerical simulations of auto-igniting mixing layers in ammonia and ammonia-hydrogen combustion under engine-relevant conditions, International Journal of Hydrogen Energy, https://doi.org/10.1016/j.ijhydene.2022.08.290

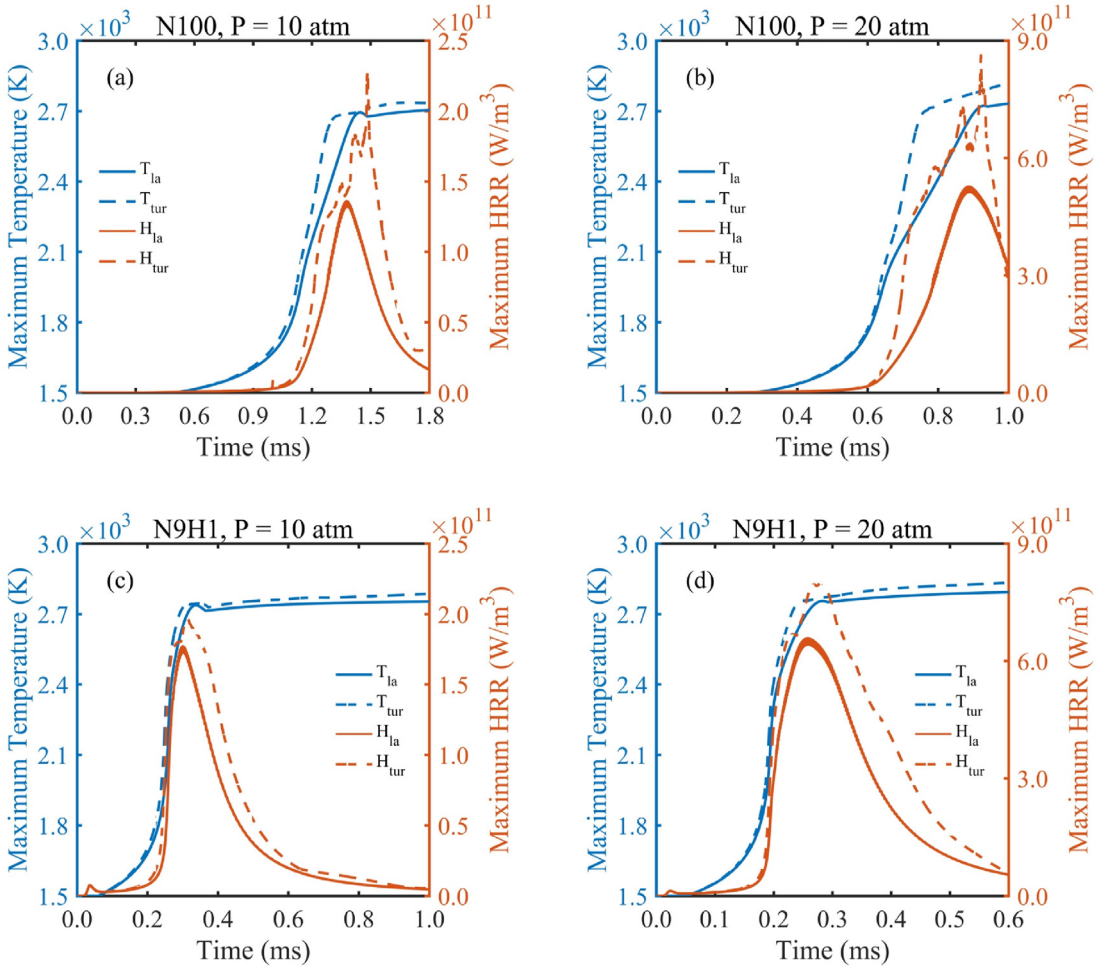

Fig. 15 – Maximum temperature and heat release rate between laminar and turbulent mixing layer simulations.

in Fig. 14 indicates the unity of Damköhler number ($Da = \tau_d/\tau_r$), which clearly separates the ignition region ($Da > 1$) and non-ignition region ($Da < 1$) [23,35]. In Fig. 14, the points extracted from the stoichiometric mixture fraction iso-lines are located in the non-ignition region, while the points from the most reactive iso-lines are in the ignition region coloured by the heat release rate values. Meanwhile, the lower reaction time means the faster reaction rate of NH_2. In the ignition region, the reaction rate increases with the increment of pressure and hydrogen addition while it is not much clear in the region along the stoichiometric mixture fraction because the ignition does not propagate into this region.

Comparison between laminar and turbulent results

This part mainly discusses the different characteristics of auto-ignition and flame development between laminar and turbulent conditions at elevated pressure. Table 3 shows the auto-ignition delay time calculated using Eq. (4) for all laminar and turbulent test cases.

In Fig. 15, we observe that turbulence accelerates the auto-ignition process. This is because turbulence promotes the mixing process between fuel and oxidizer. The gap between two different pressure conditions for the same fuel is clear, resulting in relatively lager difference in terms of temperature, heat release rate and auto-ignition delay time, especially for pure ammonia-air mixing layer cases. Under the same pressure, turbulence influences both the induction stage and the thermal runaway stage for the pure ammonia-air mixing layer, while only the thermal runaway stage is affected by the turbulence for ammonia-hydrogen-air cases, just like the pure hydrogen-air turbulent mixing layer [27]. This phenomenon may be caused by faster reaction rate in the induction stage due to hydrogen addition rather than turbulence. Meanwhile, fluctuations of maximum heat release rate with turbulence are clear at the thermal runaway stage, in which the combustion has already transformed from auto-ignition into fully flame development. The latter auto-ignition locations are holding much stronger heat release rate than the first ignition point. Another obvious difference is the effect of elevated pressure and hydrogen addition on the scalar dissipation rate in the downstream of the flame development, which is far from auto-ignition locations. Turbulence has little influence on the scalar dissipation rate along the most reactive mixture fraction compared with one-dimensional laminar cases while the totally opposite effect of pressure and hydrogen addition is shown under high turbulent intensity.

Please cite this article as: Yang W et al., Direct numerical simulations of auto-igniting mixing layers in ammonia and ammonia-hydrogen combustion under engine-relevant conditions, International Journal of Hydrogen Energy, https://doi.org/10.1016/j.ijhydene.2022.08.290

Conclusions

In this work, we investigated the auto-ignition of ammonia-air and ammonia-hydrogen-air mixing layers with fuel temperature of 300 K and hot air temperature of 1500 K at two different elevated pressure values of 10 atm and 20 atm respectively by means of direct numerical simulations. The one-dimensional laminar and two-dimensional turbulent reacting mixing layer simulations were conducted using a detailed chemistry mechanism consists of 22 species and 66 elementary reactions and a mixture-averaged transport model incorporating non-unity Lewis number effects. The study also carried out zero-dimensional homogeneous mixing simulations.

The major conclusions are summarised as follows:

1. The most reactive mixture fraction calculated by the zero-dimensional homogeneous mixing ignition reactor has been utilised to identify the mixture fraction value of auto-ignition locations in one-dimensional laminar and two-dimensional turbulent mixing layer simulations. In two-dimensional turbulent mixing layer, only the location with lower scalar dissipation rate can be ignited by exhibiting major heat release rate along the most reactive mixture fraction. The hydrogen addition and increasing pressure enhance the ignition process, reduce the auto-ignition delay time, and increase the number of auto-ignition kernels.
2. Two auto-ignition stages, the induction stage, and the thermal runaway stage can be clearly distinguished by three specific radical species, NH_2, HNO, and OH. The heat release rate is perfectly marked by the radical NH_2. The major distribution of radical HNO only appears in the lower temperature region. The radical OH merely appears and then achieves the steady state when temperature reaches its maximum value.
3. Two peaks of heat release rate are observed in the later stage of auto-ignition in both laminar and turbulent cases, where the flame propagation is moving into the fuel-rich side. One peak is located along the stoichiometric mixture fraction iso-line, which is mainly related with elementary reactions including OH, and the other one is raising the temperature, promoting the further flame propagation into the fuel-rich side.
4. The influence of elevated pressure and hydrogen addition on the auto-ignition location in both laminar and turbulent cases are consistent. Increasing pressure reduces the scalar dissipation rate while hydrogen addition increases the scalar dissipation rate due to the high diffusivity of hydrogen. This trend is observed for the whole domain of mixture fraction in the laminar mixing layer while pressure and hydrogen addition behave inversely in the downstream region of the flame development in the turbulent mixing layer.
5. The Damköhler number defined by the ratio of two-time scales between diffusion and reaction separates the ignition and non-ignition regions. The effects of pressure and hydrogen addition on reaction rate of specific radicals and diffusion level can be exhibited very well through the regime of these two-time scales.
6. The comparisons between laminar and turbulent cases show that the auto-ignition delay time is reduced by turbulence. The presence of turbulence also effects the thermal runaway stage.

Declaration of competing interest

The authors declare that they have no known competing financial interests or personal relationships that could have appeared to influence the work reported in this paper.

Acknowledgement

K. H. Luo gratefully acknowledges funding for the research and supercomputing time on ARCHER2 supported by the UK Engineering and Physical Sciences Research Council under the project "UK Consortium on Mesoscale Engineering Sciences (UKCOMES)" (Grant No. EP/R029598/1).

Appendix A. Supplementary data

Supplementary data to this article can be found online at https://doi.org/10.1016/j.ijhydene.2022.08.290.

REFERENCES

[1] Kobayashi H, Hayakawa A, Somarathne KDKA, Okafor EC. Science and technology of ammonia combustion. Proc Combust Inst 2019;37:109–33.
[2] Valera-Medina A, Xiao H, Owen-Jones M, David WIF, Bowen PJ. Ammonia for power. Prog Energy Combust Sci 2018;69:63–102.
[3] Mastorakos E. Ignition of turbulent non-premixed flames. Prog Energy Combust Sci 2009;35:57–97.
[4] Liñán A. The asymptotic structure of counterflow diffusion flames for large activation energies. Acta Astronaut 1974;1:1007–39.
[5] Fotache CG, Kreutz TG, Zhu DL, Law CK. An experimental study of ignition in nonpremixed counterflowing hydrogen versus heated air. Combust Sci Technol 1995;109:373–93.
[6] Fotache CG, Kreutz TG, Law CK. Ignition of counterflowing methane versus heated air under reduced and elevated pressures. Combust Flame 1997;108:442–70.
[7] Trujillo JYD, Kreutz TG, Law CK. Ignition in a counterflowing non-premixed CO/H_2-air system. Combust Sci Technol 1997;127:1–27.
[8] Zheng XL, Lu TF, Law CK, Westbrook CK, Curran HJ. Experimental and computational study of nonpremixed ignition of dimethyl ether in counterflow. Proc Combust Inst 2005;30:1101–9.
[9] Yu J. Asymptotic and numerical analyses of ignition of a fuel jet in a supersonic airstream. Combust Sci Technol 1995;108:47–65.
[10] Liñán A, Crespo A. An asymptotic analysis of unsteady diffusion flames for large activation energies. Combust Sci Technol 1976;14:95–117.
[11] Arndt CM, Papageorge MJ, Fuest F, Sutton JA, Meier W, Aigner M. The role of temperature, mixture fraction, and

scalar dissipation rate on transient methane injection and auto-ignition in a jet in hot coflow burner. Combust Flame 2016;167:60–71.
[12] Markides CN, Mastorakos M. Flame propagation following the autoignition of axisymmetric hydrogen, acetylene, and normal-heptane plumes in turbulent coflows of hot air. J Eng Gas Turbines Power 2008;130:011502.
[13] Markides CN, Mastorakos M. An experimental study of hydrogen autoignition in a turbulent co-flow of heated air. Proc Combust Inst 2005;30:883–91.
[14] Echekki T, Gupta KG. Hydrogen autoignition in a turbulent jet with preheated co-flow air. Int J Hydrogen Energy 2009;34:8352–77.
[15] Bhagatwala A, Luo Z, Shen H, Sutton JA, Lu T, Chen JH. Numerical and experimental investigation of turbulent DME jet flames. Proc Combust Inst 2015;35:1157–66.
[16] Echekki T, Ahmed SF. Turbulence effects on autoignition of DME in a turbulent co-flowing jet. Combust Flame 2017;178:70–81.
[17] Macfarlane RWA, Dunn M, Juddoo M, Masri A. The evolution of autoignition kernels in turbulent flames of dimethyl ether. Combust Flame 2018;197:182–96.
[18] Um DH, Joo JM, Lee S, Kwon OC. Combustion stability limits and NOx emissions of nonpremixed ammonia-substituted hydrogen-air flames. Int J Hydrogen Energy 2013;38:14854–65.
[19] Woo M, Choi BC, Ghoniem AF. Experimental and numerical studies on NOx emission characteristics in laminar non-premixed jet flames of ammonia-containing methane fuel with oxygen/nitrogen oxidizer. Energy 2016;114:961–72.
[20] Mastorakos M, Baritaud TA, Poinsot TJ. Numerical simulations of autoignition in turbulent mixing flows. Combust Flame 1997;109:198–223.
[21] Im HG, Chen JH, Law CK. Ignition of hydrogen-air mixing layer in turbulent flows. Symposium (International) on Combustion 1998;27:1047–56.
[22] Echekki T, Chen JH. High-temperature combustion in autoigniting non-homogeneous hydrogen/air mixtures. Proc Combust Inst 2002;29:2061–8.
[23] Echekki T, Chen JH. Direct numerical simulation of autoignition in non-homogeneous hydrogen-air mixtures. Combust Flame 2003;134:169–91.
[24] Hilbert R, Thévenin D. Autoignition of turbulent non-premixed flames investigated using direct numerical simulations. Combust Flame 2002;128:22–37.
[25] Chen JH, Hawkes ER, Sankaran R, Mason SD, Im HG. Direct numerical simulation of ignition front propagation in a constant volume with temperature inhomogeneities I. Fundamental analysis and diagnostics. Combust Flame 2006;145:128–44.
[26] Hawkes ER, Sankaran R, Pebay PP, Chen JH. Direct numerical simulation of ignition front propagation in a constant volume with temperature inhomogeneities II. Parametric study. Combust Flame 2006;145:145–59.
[27] Yao T, Yang WH, Luo KH. Direct numerical simulation study of hydrogen/air auto-ignition in turbulent mixing layer at elevated pressures. Comput Fluid 2018;173:59–72.
[28] Yao T, Wang Q, Luo KH. Formation and evolution of flame kernels in autoignition of a turbulent hydrogen/air mixing layer at 50 atm. Fuel 2019;255:115735.
[29] Song C, Luo K, Jin T, Wang H, Fan J. Direct numerical simulation on auto-ignition characteristics of turbulent supercritical hydrothermal flames. Combust Flame 2019;200:354–64.
[30] Jin T, Song C, Wang H, Gao Z, Luo K, Fan J. Direct numerical simulation of a supercritical hydrothermal flame in a turbulent jet. J Fluid Mech 2021;922:A8.
[31] Sreedhara S, Lakshmisha KN. Direct numerical simulation of autoignition in non-premixed, turbulent medium. Proc Combust Inst 2000;28:25–34.
[32] Sreedhara S, Lakshmisha KN. Autoignition in a non-premixed medium: DNS studies on the effects of three-dimensional turbulence. Proc Combust Inst 2002;29:2051–9.
[33] Gopalakrishnan V, Abraham J. Effects of multicomponent diffusion on predicted ignition characteristics of an n-heptane diffusion flame. Combust Flame 2004;136:557–66.
[34] Løvås T, Lowe A, Cant RS, Mastorakos M. Three-dimensional direct numerical simulations of autoignition in turbulent non-premixed flows with simple and complex chemistry. Proceedings of FEDSM2006. 2006 ASME Joint U.S.-European Fluids Engineering Summer Meeting. July 17-20, 2006 [Miami, FL].
[35] Mukhopadhyay S, Abraham J. Influence of compositional stratification on auto-ignition in n-heptane/air mixtures. Combust Flame 2011;158:1064–75.
[36] Mukhopadhyay S, Abraham J. Influence of heat release and turbulence on scalar dissipation rate in autoigniting n-heptane/air mixtures. Combust Flame 2012;159:2883–95.
[37] Krisman A, Hawkes ER, Chen JH. Two-stage autoignition and edge flames in a high pressure turbulent jet. J Fluid Mech 2017;824:5–41.
[38] van Oijen JA. Direct numerical simulation of autoigniting mixing layers in MILD combustion. Proc Combust Inst 2013;34:1163–71.
[39] Zhang H, Hawkes ER, Chen JH, Kook S. A numerical study of the autoignition of dimethyl ether with temperature inhomogeneities. Proc Combust Inst 2013;34:803–12.
[40] Bansal G, Mascarenhas A, Chen JH. Direct numerical simulations of autoignition in stratified dimethyl-ether (DME)/air turbulent mixtures. Combust Flame 2015;162:688–702.
[41] Pal P, Mansfield AB, Arias PG, Wooldrige MS, Im HG. A computational study of syngas autoignition characteristics at high-pressure and low-temperature conditions with thermal inhomogeneities. Combust Theor Model 2015;19:587–601.
[42] Im HG, Pal P, Wooldrige MS, Mansfield AB. A regime diagram for autoignition of homogeneous reactant mixtures with turbulent velocity and temperature fluctuations. Combust Sci Technol 2015;187:1263–75.
[43] Pal P, Valorani M, Arias PG, Im HG, Wooldrige MS, Ciottoli PP, Galassi RM. Computational characterization of ignition regimes in a syngas/air mixture with temperature fluctuations. Proc Combust Inst 2017;36:3705–16.
[44] Krisman A, Hawkes ER, Talei M, Bhagatwala A, Chen JH. Characterisation of two-stage ignition in diesel engine-relevant thermochemical conditions using direct numerical simulation. Combust Flame 2016;172:326–41.
[45] Krisman A, Hawkes ER, Talei M, Bhagatwala A, Chen JH. A direct numerical simulation of cool-flame affected autoignition in diesel engine-relevant conditions. Proc Combust Inst 2017;36:3567–75.
[46] Jin T, Wu Y, Wang X, Luo KH, Lu T, Luo K, Fan J. Ignition dynamics of DME/methane-air reactive mixing layer under reactivity controlled compression ignition conditions: effects of cool flames. Appl Energy 2019;249:343–54.
[47] Su L, Zhang M, Wang J, Huang Z. Direct numerical simulation of DME auto-ignition with temperature and composition stratification under HCCI engine conditions. Fuel 2021;285:119073.
[48] Rocha RC, Costa M, Bai XS. Chemical kinetic modelling of ammonia/hydrogen/air ignition, premixed flame propagation and NO emission. Fuel 2019;246:24–33.

Please cite this article as: Yang W et al., Direct numerical simulations of auto-igniting mixing layers in ammonia and ammonia-hydrogen combustion under engine-relevant conditions, International Journal of Hydrogen Energy, https://doi.org/10.1016/j.ijhydene.2022.08.290

[49] Mathieu O, Petersen EL. Experimental and modeling study on the high-temperature oxidation of ammonia and related NOx chemistry. Combust Flame 2015;162:554–70.
[50] Okafor EC, Naito Y, Colson S, Ichikawa A, Kudo T, Hayakawa A, et al. Experimental and numerical study of the laminar burning velocity of CH_4-NH_3-air premixed flames. Combust Flame 2018;187:185–98.
[51] Otomo J, Koshi M, Mitsumori T, Iwasaki H, Yamada K. Chemical kinetic modeling of ammonia oxidation with improved reaction mechanism for ammonia/air and ammonia/hydrogen/air combustion. Int J Hydrogen Energy 2018;43:3004–14.
[52] He X, Shu B, Nascimento, Moshammer K, Costa M, Fernandes RX. Auto-ignition kinetics of ammonia and ammonia/hydrogen mixtures at intermediate temperatures and high pressures. Combust Flame 2019;206:189–200.
[53] Dai L, Gersen S, Glarborg P, Mokhov A, Levinsky H. Autoignition studies of NH 3/CH 4 mixtures at high pressure. Combust Flame 2020;218:19–26.
[54] Chen J, Jiang X, Qin X, Huang Z. Effect of hydrogen blending on the high temperature auto-ignition of ammonia at elevated pressure. Fuel 2021;287:119563.
[55] Somarathne KDKA, Okafor EC, Hayakawa A, Kudo T, Kurata O, Iki N, Kobayashi H. Emission characteristics of turbulent non-premixed ammonia/air and methane/air swirl flames through a rich-lean combustor under various wall thermal boundary conditions at high pressure. Combust Flame 2019;210:247–61.
[56] Somarathne KDKA, Okafor EC, Sugawara D, Hayakawa A, Kobayashi H. Effects of OH concentration and temperature on NO emission characteristics of turbulent non-premixed CH_4/NH_3/air flames in a two-stage gas turbine like combustor at high pressure. Proc Combust Inst 2021;38:5163–70.
[57] Thévenin D, Behrendt F, Maas U, Przywara B, Warnatz J. Development of a parallel direct simulation code to investigate reactive flows. Comput Fluid 1996;25:485–96.
[58] Poinsot T, Lele S. Boundary conditions for direct simulations of compressible viscous flows. J Comput Phys 1992;101:104–29.
[59] Kempf A, Klein M, Janicka J. Efficient generation of initial and inflow conditions for transient flows in arbitrary geometries. Flow, Turbul Combust 2005;74:67–84.
[60] Thévenin D, Fru G, Janiga G. Direct numerical simulations of the impact of high turbulence intensities and volume viscosity on premixed methane flames. Journal of Combustion 2011;2011. Article ID 746719.
[61] Fru G, Thévenin D, Janiga G. Impact of turbulence intensity and equivalence ratio on the burning rate of premixed methane-air flames. Energies 2011;4:878–93.
[62] Ranga Dinesh Kkj, Shalaby H, Luo KH, van Oijen JA, Thévenin D. High hydrogen content syngas fuel burning in lean premixed spherical flames at elevated pressures: effects of preferential diffusion. Int J Hydrogen Energy 2016;41:18231–49.
[63] Ranga Dinesh Kkj, Shalaby H, Luo KH, van Oijen JA, Thévenin D. Effects of pressure on cellular flame structure of high hydrogen content lean premixed syngas spherical flames: a DNS study. Int J Hydrogen Energy 2016;41:21516–31.
[64] Ranga Dinesh Kkj, Shalaby H, Luo KH, van Oijen JA, Thévenin D. Heat release rate variations in high hydrogen content premixed syngas flames at elevated pressures: effect of equivalence ratio. Int J Hydrogen Energy 2017;42:7029–44.
[65] Yang W, Ranga Dinesh Kkj, Luo KH, Thévenin D. Direct numerical simulation of turbulent premixed ammonia and ammonia-hydrogen combustion under engine-relevant conditions. Int J Hydrogen Energy 2022;47:11083–100.
[66] Netzer C, Ahmed A, Gruber A, Lovas T. Curvature effects on NO formation in wrinkled laminar ammonia/hydrogen/nitrogen-air premixed flames. Combust Flame 2021;232:111520.
[67] Bilger RW. The structure of turbulent nonpremixed flames. Symposium (International) on Combustion 1989;22:475–88.
[68] Goodwin DG, Moffat HK, Speth RL. Cantera: an object-oriented software toolkit for chemical kinetics, thermodynamics, and transport processes. 2021. version 2.4.0, http://www.cantera.org.

Please cite this article as: Yang W et al., Direct numerical simulations of auto-igniting mixing layers in ammonia and ammonia-hydrogen combustion under engine-relevant conditions, International Journal of Hydrogen Energy, https://doi.org/10.1016/j.ijhydene.2022.08.290